(+)- and *ent*-(−)-Duocarmycin SA and (+)- and *ent*-(−)-*N*-BOC-DSA DNA Alkylation Properties. Alkylation Site Models That Accommodate the Offset AT-Rich Adenine N3 Alkylation Selectivity of the Enantiomeric Agents

Dale L. Boger,* Douglas S. Johnson,† and Weiya Yun

Contribution from the Department of Chemistry, The Scripps Research Institute, 10666 North Torrey Pines Road, La Jolla, California 92037

Received September 17, 1993®

Abstract: A detailed study of the DNA alkylation properties of (+)-duocarmycin SA, *ent*-(−)-duocarmycin SA, and (+)- and *ent*-(−)-*N*-BOC-DSA (**2**) is described, and the development of a model that accommodates the offset AT-rich adenine N3 alkylation selectivity of the enantiomeric agents is presented.

Two independent efforts have described the isolation, structure determination, assignment of absolute configuration, and preliminary evaluation of the initial members of a new class of exceptionally potent antitumor antibiotics including duocarmycin A (**3**),[1-3] duocarmycin B_1-B_2,[5] and duocarmycin C_1-C_2[2-4] (pyrindamycin B and A).[6] Subsequent to their disclosure, we described the event,[7] sequence selectivity,[8] quantitation,[9] reversibility,[10] and unambiguous establishment of the structure of the product[9] of the adenine N3 DNA alkylation reaction for duocarmycin A and C_1-C_2 which provided the necessary information for development of an accurate model[8,11,12] of the predominant DNA alkylation event. In these studies, the major DNA alkylation reaction (86–92%) was shown to proceed by 3′ adenine N3 addition to the less substituted cyclopropane carbon preferentially within selected, four base-pair (bp) AT-rich minor groove sites (5′-AA<u>A</u> > 5′-TT<u>A</u> ≫ 5′-TA<u>A</u> > 5′-AT<u>A</u>) with an agent binding orientation in the minor groove that extends in the 3′→5′ direction from the alkylation site covering 3.5 base-pairs. A subsequent comparative examination[13] of (+)-duocarmycin A (**3**) with *epi*-(+)-duocarmycin A and their unnatural enantiomers[14] revealed that the productive DNA alkylation properties were embodied in the natural enantiomers (≥100 times more effective) and the *epi*-(+)-duocarmycin A exhibited the same sequence selectivity as (+)-duocarmycin A but a diminished (3–6 times lower) DNA alkylation efficiency.

Independent studies within an isolated site of an oligonucleotide have confirmed the nature of the adenine N3 alkylation within intact duplex DNA[15] and have established the accuracy of the binding model and the minor groove binding orientation.[16] Additional recent studies with oligonucleotides lacking a high-affinity alkylation site have established a minor guanine N3 alkylation event.[17] Further studies of this alternative guanine N3 alkylation have shown that it is observed only when adenine alkylation sites within AT-rich regions of labeled restriction fragments are not available, when the DNA alkylation reaction is conducted with a large excess of agent, or when the adenine alkylation sites within AT-rich regions were prebound and protected with high affinity AT-rich minor groove binding agents including distamycin A.[18] Inherent in this work was the verification of the prominent role that noncovalent binding selectivity[19] plays in contributing to the sequence selective DNA alkylation reaction.[11,12]

(+)-Duocarmycin SA (**1**),[20] an exceptionally potent antitumor antibiotic isolated in trace quantities from *Streptomyces* sp. DO113 (0.01 mg/L) and first described in 1990, constitutes the newest and most potent[21] member of this growing class of agents. Because of its enhanced solvolytic stability[21] and biological potency relative to its predecessors including (+)-duocarmycin A (**3**),

† Recipient of a Graduate Fellowship from the Organic Division of the American Chemical Society sponsored by ZENECA Pharmaceuticals, 1993–94.

® Abstract published in *Advance ACS Abstracts*, February 1, 1994.

(1) Duocarmycin A: Takahashi, I.; Takahashi, K.; Ichimura, M.; Morimoto, M.; Asano, K.; Kawamoto, I.; Tomita, F.; Nakano, H. *J. Antibiot.* **1988**, *41*, 1915.

(2) Yasuzawa, T.; Iida, T.; Muroi, K.; Ichimura, M.; Takahashi, K.; Sano, H. *Chem. Pharm. Bull.* **1988**, *36*, 3728.

(3) DC89-A1 (duocarmycin C_1) and DC88-A (duocarmycin A): Nakano, H.; Takahashi, I.; Ichimura, M.; Kawamoto, I.; Asano, K.; Tomita, F.; Sano, H.; Yasuzawa, T.; Morimoto, M.; Fujimoto, K. PCT Int. Appl. WO87 06265, 1987; *Chem. Abstr.* **1988**, *108*, 110858s.

(4) DC89-A1: Ichimura, M.; Muroi, K.; Asano, K.; Kawamoto, I.; Tomita, F.; Morimoto, M.; Nakano, H. *J. Antibiot.* **1988**, *41*, 1285.

(5) Duocarmycin B_1 and B_2: Ogawa, T.; Ichimura, M.; Katsumata, S.; Morimoto, M.; Takahashi, K. *J. Antibiot.* **1989**, *42*, 1299.

(6) Pyrindamycin A and B: Ohba, K.; Watabe, H.; Sasaki, T.; Takeuchi, Y.; Kodama, Y.; Nakazawa, T.; Yamamoto, H.; Shomura, T.; Sezaki, M.; Kondo, S. *J. Antibiot.* **1988**, *41*, 1515. Ishii, S.; Nagasawa, M.; Kariya, Y.; Yamamoto, H.; Inouye, S.; Kondo, S. *J. Antibiot.* **1989**, *42*, 1713.

(7) Boger, D. L.; Ishizaki, T.; Zarrinmayeh, H.; Kitos, P. A.; Suntornwat, O. *J. Org. Chem.* **1990**, *55*, 4499.

(8) Boger, D. L.; Ishizaki, T.; Zarrinmayeh, H.; Munk, S. A.; Kitos, P. A.; Suntornwat, O. *J. Am. Chem. Soc.* **1990**, *112*, 8961.

(9) Boger, D. L.; Ishizaki, T.; Zarrinmayeh, H. *J. Am. Chem. Soc.* **1991**, *113*, 6645.

(10) Boger, D. L.; Yun, W. *J. Am. Chem. Soc.* **1993**, *115*, 9872.

(11) (a) Boger, D. L. *Chemtracts: Org. Chem.* **1991**, *4*, 329. (b) Boger, D. L. In *Advances in Heterocyclic Natural Products Synthesis*, Vol. 2; Pearson, W. H., Ed.; JAI Press: Greenwich, CT, 1992; pp 1–188.

(12) Boger, D. L. In *Proc. R. A. Welch Foundation Conf. Chem. Res., Chem. Front. Med.* **1991**, *35*, 137.

(13) Boger, D. L.; Yun, W.; Terashima, S.; Fukuda, Y.; Nakatani, K.; Kitos, P. A.; Jin, Q. *Bioorg. Med. Chem. Lett.* **1992**, *2*, 759.

(14) For the total synthesis of duocarmycin A, see: Fukuda, Y.; Nakatani, K.; Terashima, S. *Bioorg. Med. Chem. Lett.* **1992**, *2*, 755. Fukuda, Y.; Nakatani, K.; Ito, Y.; Terashima, S. *Tetrahedron Lett.* **1990**, *31*, 6699.

(15) Sugiyama, H.; Hosoda, M.; Saito, I.; Asai, A.; Saito, H. *Tetrahedron Lett.* **1990**, *31*, 7197.

(16) Lin, C. H.; Patel, D. J. *J. Am. Chem. Soc.* **1992**, *114*, 10658.

(17) Sugiyama, H.; Ohmori, K.; Chan, K. L.; Hosoda, M.; Asai, A.; Saito, H.; Saito, I. *Tetrahedron Lett.* **1993**, *34*, 2179.

(18) Yamamoto, K.; Sugiyama, H.; Kawanishi, S. *Biochemistry* **1993**, *32*, 1059.

(19) Boger, D. L.; Invergo, B. J.; Coleman, R. S.; Zarrinmayeh, H.; Kitos, P. A.; Thompson, S. C.; Leong, T.; McLaughlin, L. W. *Chem.-Biol. Interact.* **1990**, *73*, 29. Boger, D. L.; Sakya, S. M. *J. Org. Chem.* **1992**, *57*, 1277. Boger, D. L.; Coleman, R. S.; Invergo, B. J. *J. Org. Chem.* **1987**, *52*, 1521. Boger, D. L.; Coleman, R. S. *J. Org. Chem.* **1984**, *49*, 2240.

(20) Ichimura, M.; Ogawa, T.; Takahashi, K.; Kobayashi, E.; Kawamoto, I.; Yasuzawa, T.; Takahashi, I.; Nakano, H. *J. Antibiot.* **1990**, *43*, 1037. Ichimura, M.; Ogawa, T.; Katsumata, S.; Takahashi, K.; Takahashi, I.; Nakano, H. *J. Antibiot.* **1991**, *44*, 1045.

(21) Boger, D. L.; Machiya, K.; Hertzog, D. L.; Kitos, P. A.; Holmes, D. *J. Am. Chem. Soc.* **1993**, *115*, 9025. Boger, D. L.; Machiya, K. *J. Am. Chem. Soc.* **1992**, *114*, 10056. Boger, D. L. *Pure Appl. Chem.* **1993**, *65*, 1123.

0002-7863/94/1516-1635$04.50/0

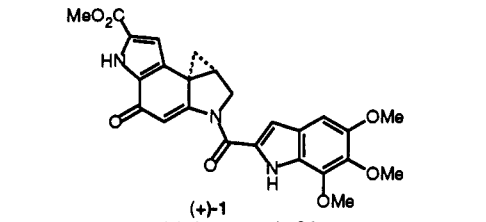

(+)-1
(+)-duocarmycin SA

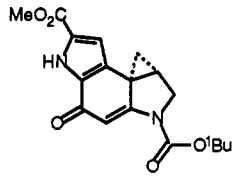

(+)-2
(+)-N-BOC DSA

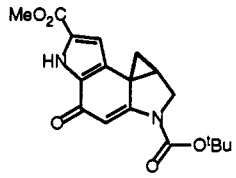

(-)-2
(-)-N-BOC DSA

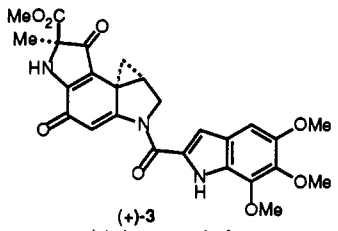

(+)-3
(+)-duocarmycin A

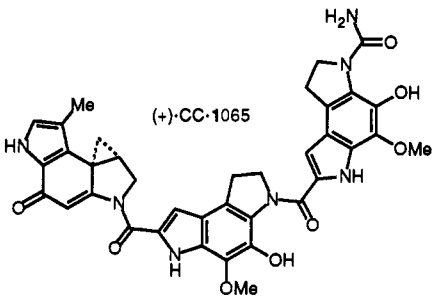

(+)-CC-1065

(+)-CC-1065,[11,22-31] and structurally related agents,[32-34] the examination of (+)-**1**, its unnatural enantiomer, and structurally related agents including (+)- and *ent*-(−)-**2** promised to be especially important.

Herein, we report a complete and detailed study of the DNA alkylation properties of (+)-duocarmycin SA, *ent*-(−)-duocarmycin SA, and both enantiomers of *N*-BOC-DSA (**2**), a simple derivative of the alkylation subunit. Notably, the natural product has not been made available for such studies because of the limited supply.[35] The studies detailed herein were conducted with materials secured by chemical synthesis,[21] which provided not only (+)-**1** but also (+)-**2** and the corresponding unnatural enantiomers. In addition to constituting the first disclosure of the event, sequence selectivity, quantitation, reversibility, and unambiguous structural confirmation of the product of the duplex DNA minor groove adenine N3 alkylation by natural (+)-duocarmycin SA, Scheme 1, these studies constitute the first disclosure of DNA alkylation by a duocarmycin unnatural enantiomer.

DNA Alkylation Studies. The DNA alkylation properties of the agents were examined within five 150 base-pair segments of duplex DNA for which comparative results are available for related agents including (+)-duocarmycin A and (+)-CC-1065. Five clones of phage M13mp10 were selected for study and contain SV40 nucleosomal DNA inserts: w794 (nucleotide no. 5238-138) and its complement w836 (nucleotide no. 5189-91), c988 (nucleotide no. 4359-4210) and its complement c820 (nucleotide no. 4196-4345), and c1346 (nucleotide no. 1632-1782).[29] The alkylation site identification and the assessment of the relative selectivity among the available sites was obtained by thermally-induced strand cleavage of the singly 5′ end-labeled duplex DNA after exposure to the agents. Following treatment of the end-labeled duplex DNA with a range of agent concentrations (24 h, 4–37 °C), the unbound agent was removed by EtOH precipitation of the DNA. Redissolution of the DNA in aqueous buffer, thermolysis (100 °C, 30 min) to induce strand cleavage at the sites of DNA alkylation, denaturing high-resolution polyacrylamide gel electrophoresis (PAGE) adjacent to Sanger dideoxynucleotide sequencing standards,[36] and autoradiography led to identification of the DNA cleavage and alkylation sites. It was established in our studies that rapid thermolysis at 100 °C at neutral to low pH (pH 6–7) and at low salt concentration minimizes the potentially competitive reversible DNA alkylation reaction and optimizes thermal depurination, leading to stoichiometric strand cleavage at the sites of DNA alkylation. Thermal depurination conducted at lower temperatures (50–90 °C), at higher pH (8.0), and, to a lesser extent, at high ionic strength favored reversal of the DNA alkylation reaction attributable to base-catalyzed phenol deprotonation required of retroalkylation and maintenance of duplex (favors retroalkylation) versus denatured (favors depurination) DNA.

The full details of this procedure have been disclosed and discussed elsewhere.[29] However, since it differs from the

(22) Warpehoski, M. A. In *Advances in DNA Sequence Specific Agents*; Hurley, L. H., Ed.; JAI Press: Greenwich, CT, 1992; Vol. 1, p 217. Warpehoski, M. A.; Hurley, L. H. *Chem. Res. Toxicol.* **1988**, *1*, 315. Hurley, L. H.; Draves, P. H. In *Molecular Aspects of Anticancer Drug–DNA Interactions*; Neidle, S., Waring, M., Eds.; CRC Press: Ann Arbor, MI, 1993; Vol. 1, p 89. Hurley, L. H.; Needham-VanDevanter, D. R. *Acc. Chem. Res.* **1986**, *19*, 230.

(23) Coleman, R. S.; Boger, D. L. In *Studies in Natural Product Chemistry* Vol. 3; Atta-ur-Rahman, Ed.; Elsevier: Amsterdam, 1989; p 301.

(24) Hurley, L. H.; Reynolds, V. L.; Swenson, D. H.; Petzold, G. L.; Scahill, T. A. *Science* **1984**, *226*, 843.

(25) Scahill, T. A.; Jensen, R. M.; Swenson, D. H.; Hatzenbuhler, N. T.; Petzold, G.; Wierenga, W.; Brahme, N. D. *Biochemistry* **1990**, *29*, 2852. Lin, C. H.; Hurley, L. H. *Biochemistry* **1990**, *29*, 9503.

(26) Hurley, L. H.; Lee, C.-S.; McGovren, J. P.; Warpehoski, M. A.; Mitchell, M. A.; Kelly, R. C.; Aristoff, P. A. *Biochemistry* **1988**, *27*, 3886.

(27) Hurley, L. H.; Warpehoski, M. A.; Lee, C.-S.; McGovren, J. P.; Scahill, T. A.; Kelly, R. C.; Mitchell, M. A.; Wicnienski, N. A.; Gebhard, I.; Johnson, P. D.; Bradford, V. S. *J. Am. Chem. Soc.* **1990**, *112*, 4633.

(28) Boger, D. L.; Coleman, R. S.; Invergo, B. J.; Sakya, S. M.; Ishizaki, T.; Munk, S. A.; Zarrinmayeh, H.; Kitos, P. A.; Thompson, S. C. *J. Am. Chem. Soc.* **1990**, *112*, 4623. For the development of comparable alkylation site models that accommodate the offset AT-rich adenine N3 alkylation selectivity of (+)-CC-1065 and *ent*-(−)-CC-1065 and related agents, see: Boger, D. L.; Johnson, D. S.; Yun, W.; Tarby, C. *Bioorg. Med. Chem.*, in press. Boger, D. L.; Coleman, R. S. *J. Am. Chem. Soc.* **1988**, *110*, 4796 and 1321.

(29) Boger, D. L.; Munk, S. A.; Zarrinmayeh, H.; Ishizaki, T.; Haught, J.; Bina, M. *Tetrahedron* **1991**, *47*, 2661.

(30) Boger, D. L.; Munk, S. A.; Ishizaki, T. *J. Am. Chem. Soc.* **1991**, *113*, 2779.

(31) Boger, D. L.; Munk, S. A.; Zarrinmayeh, H. *J. Am. Chem. Soc.* **1991**, *113*, 3980.

(32) CI-based analogs: Boger, D. L.; Zarrinmayeh, H.; Munk, S. A.; Kitos, P. A.; Suntornwat, O. *Proc. Natl. Acad. Sci. U.S.A.* **1991**, *88*, 1431. Synthesis: Boger, D. L.; Wysocki, R. J., Jr. *J. Org. Chem.* **1989**, *54*, 1238. Boger, D. L.; Wysocki, R. J., Jr.; Ishizaki, T. *J. Am. Chem. Soc.* **1990**, *112*, 5230. Drost, K. J.; Jones, R. J.; Cava, M. P. *J. Org. Chem.* **1989**, *54*, 5985. Tidwell, J. H.; Buchwald, S. L. *J. Org. Chem.* **1992**, *57*, 6380. Wang, Y.; Lown, J. W. *Heterocycles* **1993**, *36*, 1399. Sundberg, R. J.; Baxter, E. W. *Tetrahedron Lett.* **1986**, *27*, 2687.

(33) CBI-based analogs: Boger, D. L.; Munk, S. A. *J. Am. Chem. Soc.* **1992**, *114*, 5487. Synthesis: Boger, D. L.; Ishizaki, T.; Wysocki, R. J., Jr.; Munk, S. A.; Kitos, P. A.; Suntornwat, O. *J. Am. Chem. Soc.* **1989**, *111*, 6461. Boger, D. L.; Ishizaki, T.; Kitos, P. A.; Suntornwat, O. *J. Org. Chem.* **1990**, *55*, 5823. Boger, D. L.; Ishizaki, T. *Tetrahedron Lett.* **1990**, *31*, 793. Boger, D. L.; Ishizaki, T.; Zarrinmayeh, H.; Kitos, P. A.; Suntornwat, O. *Bioorg. Med. Chem. Lett.* **1991**, *1*, 55. Boger, D. L.; Ishizaki, T.; Sakya, S. M.; Munk, S. A.; Kitos, P. A.; Jin, Q.; Besterman, J. M. *Bioorg. Med. Chem. Lett.* **1991**, *1*, 115. Drost, K. J.; Cava, M. P. *J. Org. Chem.* **1991**, *56*, 2240. Boger, D. L.; Yun, W.; Teegarden, B. R. *J. Org. Chem.* **1992**, *57*, 2873. Aristoff, P. A.; Johnson, P. D. *J. Org. Chem.* **1992**, *57*, 6234. Aristoff, P. A.; Johnson, P. D.; Sun, D. *J. Med. Chem.* **1993**, *36*, 1956.

(34) C_2BI-based analogs: Boger, D. L.; Palanki, M. S. S. *J. Am. Chem. Soc.* **1992**, *114*, 9318. Boger, D. L.; Johnson, D. S.; Palanki, M. S. S.; Kitos, P. A.; Chang, J.; Dowell, P. *Bioorg. Med. Chem.* **1993**, *1*, 27.

(35) (+)-Duocarmycin SA derived from natural soruces was not available for study; personal communication: H. Saito, Kyowa Hakko Kogyo, Ltd., Tokyo, Japan. The materials used for the studies detailed herein were prepared by chemical synthesis, ref 21.

(36) Sanger, F.; Nicklen, S.; Coulsen, A. R. *Proc. Natl. Acad. Sci. U.S.A.* **1977**, *74*, 5463.

Scheme 1

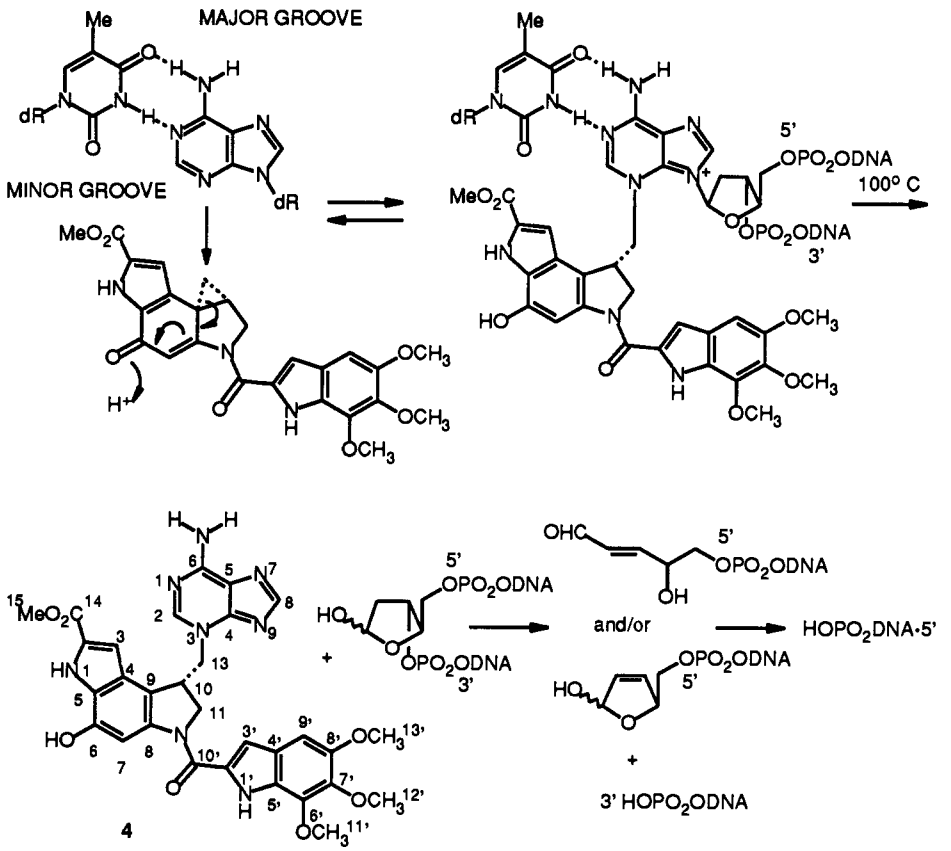

conventional use of an end-labeled restriction fragment, a few features of the procedure merit highlighting. Although there are a number of technical advantages to the procedure, the most prominent is that it requires less than 24 h to prepare unlimited quantities of end-labeled duplex DNA for binding studies and complete Sanger[36] sequencing (G, C, A, and T) is performed on the template concurrent with the enzymatic synthesis of the end-labeled DNA. This avoids the requirement of conducting the labor-intensive Maxam–Gilbert chemical cleavage reactions for the preparation of sequencing standards (G and G + A) as is required with the use of restriction fragments.[37] Moreover, even moderate care in reproducing the conditions for the enzymatic labeled primer–template extension reaction dependably provides sufficient unlabeled duplex DNA liberated in the final restriction enzyme cleavage to reproducibly serve as carrier duplex DNA (ca. 10 times the amount of labeled DNA.)

The thermal treatment of the agent-alkylated DNA results in depurination and strand cleavage at the site of alkylation, while the Sanger sequencing reactions result in base incorporation but halted chain elongation at the sequenced site. Consequently, cleavage at nucleotide N (sequencing) represents alkylation at nucleotide N + 1. The gel legends included herein identify the alkylation sites. The 3′ end heterogeneity in the gels (double bands) observed with the 5′ end-labeled DNA constitutes a single alkylation site. The band observed at higher molecular weight (lower gel mobility) constitutes a thermal cleavage product containing a modified sugar, presumably the aldehyde or hemiacetal form of 2,3-dehydro-2,3-dideoxyribose. The second band at lower molecular weight (higher gel mobility) constitutes the subsequent β-elimination product with loss of the 3′ modified sugar, which results in DNA containing a 3′-phosphate at the 5′ side of the strand break. This end heterogeneity may be removed by piperidine treatment, providing a single cleavage product constituting the lower molecular weight band which comigrates with DNA derived from the Maxam–Gilbert adenine reaction.

(37) Maxam, A. M.; Gilbert, W. *Proc. Natl. Acad. Sci. U.S.A.* **1977**, *74*, 560.

In the conduct of the work it was further demonstrated that the thermal treatment of the agent-alkylated DNA for longer than 30 min at 100 °C does not lead to additional cleavage.

Electrophoresis of the agent-treated DNA was conducted under conditions that maximize the resolution of the SV40 DNA examined. Not shown on the gels is the remaining 5′ end 55 base-pairs derived from the M13mp10 DNA. This carefully chosen 55 base-pair region contains a single alkylation site for the agents adjacent to the 5′ end-label. The apparent complete consumption of radioactivity on the gels at high agent concentrations constitutes complete cleavage of the duplex DNA at this site. The competitive cleavage at this site does not affect the relative selectivity of the examined agent within the SV40 DNA, especially at the relevant low agent concentrations constituting single alkylation events on the DNA, but it does ensure that multiple alkylations at high agent concentrations result in cleavage to a single short fragment that is not examined on the gel. This ensures that the commonly encountered gel fade to a single short fragment of 5′ end-labeled DNA at high agent concentrations is not misrepresented as increasing selectivity. Thus, built into the protocol are features that permit the identification of high affinity alkylation sites detected at the lowest agent concentrations and lower affinity alkylation sites detected at the higher agent concentrations. The use of a 10-fold amount of carrier unlabeled DNA in the binding assays permits the use of easily measured substantial changes in the agent concentration (10-fold) to effect small changes in the relative concentrations of agent and labeled DNA.

The statistical treatment of the alkylation sites provided herein proved more revealing than a conventional analysis that considers only the observed alkylation sites. That is, an evaluation that includes the consideration of sites *not* alkylated helped distinguish the composite consensus sequence and highlighted subtle features not apparent from a simple examination of the alkylated sites.

The DNA alkylation reaction selectivities observed under the incubation conditions of 37 °C (24 h) for the BOC derivatives of the alkylation subunits and 4 or 25 °C (24 h) for duocarmycin

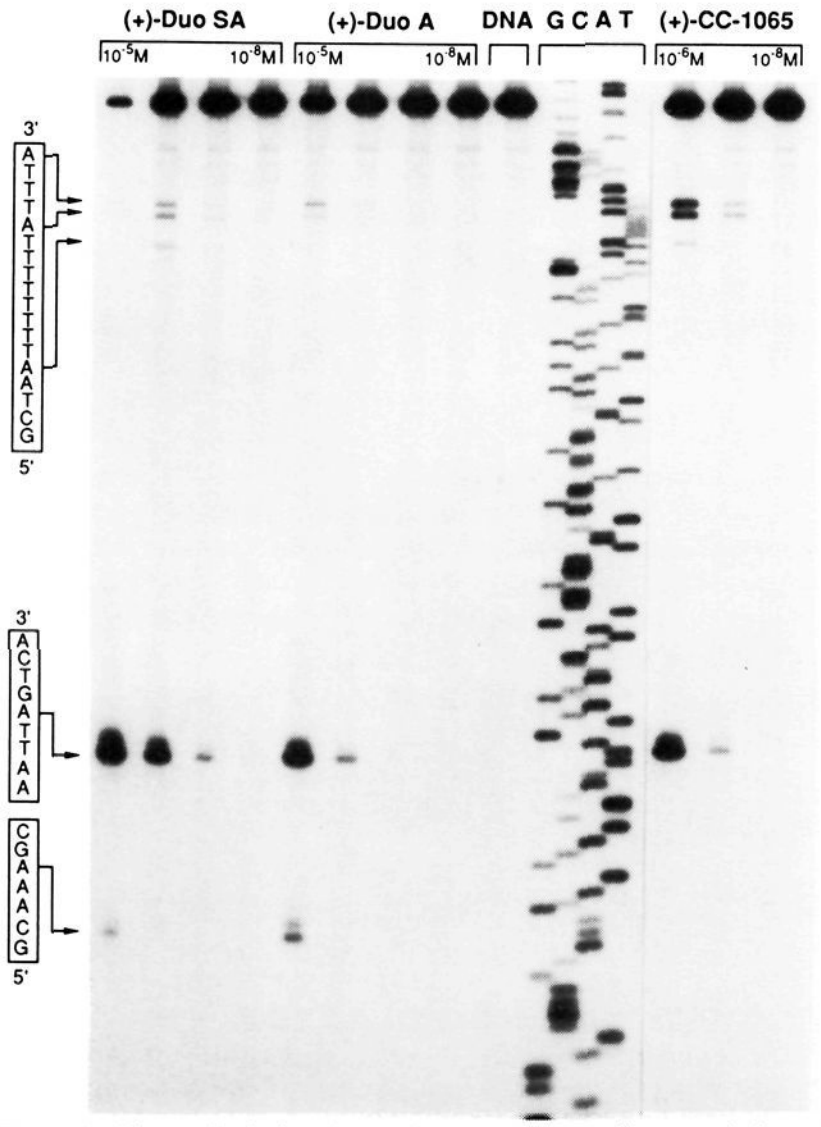

Figure 1. Thermally-induced strand cleavage of double-stranded DNA (SV40 DNA fragment, 144 bp, nucleotide no. 5238-138, clone w794) after 24 h incubation of agent–DNA at 25 °C followed by removal of unbound agent and 30 min incubation at 100 °C; 8% denaturing PAGE and autoradiography. Lanes 1–4, (+)-duocarmycin SA (1×10^{-5} to 1×10^{-8} M); lanes 5–8, (+)-duocarmycin A (1×10^{-5} to 1×10^{-8} M); lane 9, control DNA; lanes 10–13, Sanger G, C, A, and T reactions; lanes 14–16, (+)-CC-1065 (1×10^{-6} to 1×10^{-8} M).

SA have proven identical to the alkylation selectivities observed with shorter or extended reaction periods (37 or 25 °C, 0.5–7 days). In addition, the selectivity of the DNA alkylation observed under conditions of 25 or 37 °C (24–48 h) for duocarmycin SA, duocarmycin A, and (+)-CC-1065 has not proven distinguishable from that observed at 4 °C.

(+)-Duocarmycin SA. A comparison of the DNA alkylation profile for (+)-duocarmycin SA (**1**) with those of (+)-duocarmycin A (**3**) and (+)-CC-1065 within w794 DNA is illustrated in Figure 1 and is representative of that found within all segments of duplex DNA examined. Under the conditions of the assay (25 °C, 24 h), (+)-duocarmycin SA detectably alkylated DNA at concentrations as low as 10^{-7}–10^{-8} M and with essentially the same efficiency as (+)-CC-1065. It proved to be 10 times more efficient than (+)-duocarmycin A (**3**), which at 25 °C provided detectable alkylation at 10^{-6}–10^{-7} M. Unlike (+)-duocarmycin SA (**1**), for which the same efficiency of DNA alkylation within w794 DNA was observed at 4 or 25 °C (24 h), the alkylation efficiency of (+)-duocarmycin A (**3**) *increased* with a decreased incubation temperature.[8] Consistent with the relative reactivity of the three agents, this is presumably the consequence of (+)-(**1**) and (+)-CC-1065 being stable to the conditions of the assay, while (+)-**3** is of limited stability and undergoes nonproductive competitive solvolysis at the higher incubation temperatures.

Figure 2 summarizes the observed alkylation sites for the agents examined, and no significant distinctions in the sites of DNA alkylation could be found for (+)-**1** versus (+)-**3**. However, the relative selectivity of alkylation among the available sites proved to be greater with (+)-duocarmycin SA versus (+)-duocarmycin A. Characteristic of this enhanced selectivity, (+)-duocarmycin SA alkylates the minor w794 site (5′-CAAAG) only at concentrations 100–1000 times greater than that required for alkylation of the major 5′-AATTA site. In contrast, (+)-duocarmycin A more prominently alkylates this minor site,requiring concentrations only 10 times that required for alkylation at the major 5′-AATTA site, Figure 1. This enhanced selectivity is most likely attributable to the diminished chemical reactivity of (+)-duocarmycin SA. Table 1 summarizes the (+)-duocarmycin SA DNA alkylation sites and the statistical treatment that was used to determine the relative selectivity among the available alkylation sites. Without exception, *all* alkylation sites for (+)-**1** proved to be adenine under the conditions of the assay and no minor guanine alkylation was detected.[17,18] In addition, *each* adenine alkylation site was flanked by two 5′ A or T bases, and there proved to be a preference for the three base-pair sequence that follows the order of 5′-AAA > 5′-TTA > 5′-TAA > 5′-ATA. There was also a preference but not an absolute requirement for the fourth 5′ base to be A or T, and this preference was observed in most of

Table 1. Summary of DNA Alkylation Sites for (+)-Duocarmycin SA

sequence	no. total sites	no. alkylation sites
Three Base-Pair Selectivity		
5′-(NAAN)-3′	83	35 (42%)
5′-(AAAN)-3′	39	29 (74%)
5′-(TAAN)-3′	19	6 (32%)
5′-(GAAN)-3′	11	0 (00%)
5′-(CAAN)-3′	14	0 (00%)
5′-(NAAPu)-3′	54	30 (55%)
5′-(NAAPy)-3′	29	5 (17%)
5′-(NTAN)-3′	53	15 (28%)
5′-(TTAN)-3′	19	10 (53%)
5′-(ATAN)-3′	18	5 (28%)
5′-(GTAN)-3′	7	0 (00%)
5′-(CTAN)-3′	9	0 (00%)
5′-(NTAPu)-3′	29	6 (21%)
5′-(NTAPy)-3′	24	9 (38%)

sequence	no. AS/no. TS[a]	high affinity[b]	low affinity[b]
5′-(NAAAN)-3′	29/39 (74%)	24 (62%)	5
5′-(NTTAN)-3′	10/19 (53%)	2 (11%)	8
5′-(NTAAN)-3′	6/19 (32%)	2 (11%)	4
5′-(NATAN)-3′	5/18 (28%)	2 (11%)	3
5′-(NAAAN)-3′			
5′-(AAAAN)-3′	18/21 (86%)	16 (76%)	2
5′-(TAAAN)-3′	4/6 (67%)	2 (33%)	2
5′-(GAAAN)-3′	4/5 (80%)	4 (80%)	0
5′-(CAAAN)-3′	3/7 (43%)	2 (29%)	1
5′-(NAAAPu)-3′	25/30 (83%)	22 (73%)	3
5′-(NAAAPy)-3′	4/9 (44%)	2 (22%)	2
5′-(NTTAN)-3′			
5′-(ATTAN)-3′	4/4 (100%)	2 (50%)	2
5′-(TTTAN)-3′	5/6 (83%)	0 (00%)	5
5′-(GTTAN)-3′	1/5 (20%)	0 (00%)	1
5′-(CTTAN)-3′	0/4 (00%)	0 (00%)	0
5′-(NTTAPu)-3′	3/6 (50%)	2 (33%)	1
5′-(NTTAPy)-3′	7/13 (54%)	0 (00%)	7
5′-(NTAAN)-3′			
5′-(ATAAN)-3′	3/9 (33%)	1 (11%)	2
5′-(TTAAN)-3′	1/3 (33%)	0 (00%)	1
5′-(GTAAN)-3′	1/4 (25%)	1 (25%)	0
5′-(CTAAN)-3′	1/3 (33%)	0 (00%)	1
5′-(NTAAPu)-3′	4/9 (44%)	2 (22%)	2
5′-(NTAAPy)-3′	2/10 (20%)	0 (00%)	2
5′-(NATAN)-3′			
5′-(AATAN)-3′	4/5 (80%)	2 (40%)	2
5′-(TATAN)-3′	1/6 (17%)	0 (00%)	1
5′-(GATAN)-3′	0/0	0 (00%)	0
5′-(CATAN)-3′	0/7 (00%)	0 (00%)	0
5′-(NATAPu)-3′	3/14 (21%)	1 (07%)	2
5′-(NATAPy)-3′	2/4 (50%)	0 (00%)	2

[a] Number of alkylated sites/number of total sites. [b] Intensity of alkylation at the sites; high = high affinity site observed at lowest agent concentration; low = low affinity site observed at higher agent concentrations. The expressed percentage is that of the number of high affinity alkylation sites per number of total sites.

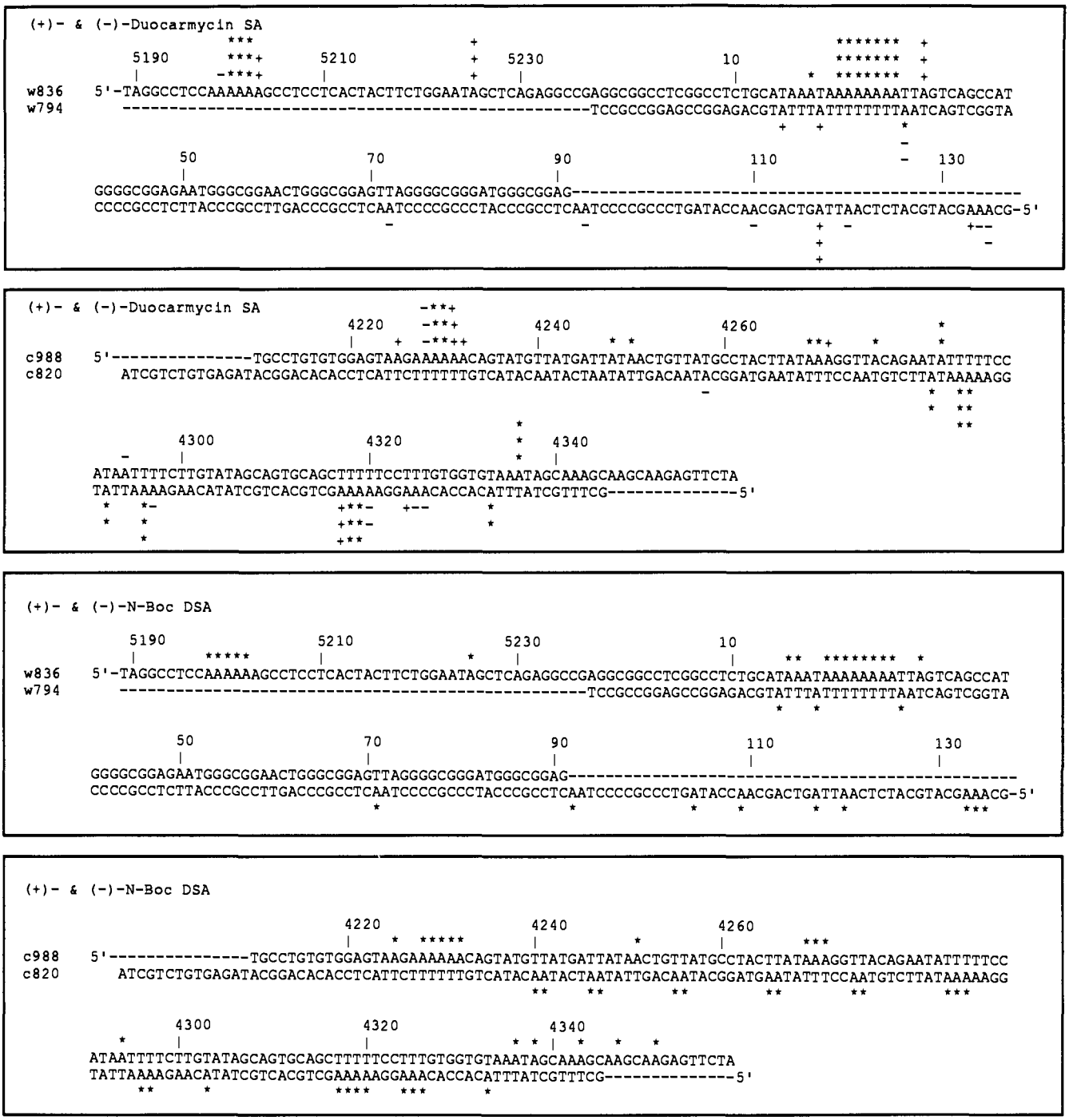

Figure 2. Summary of alkylation and cleavage sites for (+)- and (–)-duocarmycin SA and (+)- and (–)-*N*-BOC-DSA. + denotes cleavage by the natural enantiomer only; – denotes cleavage by the unnatural enantiomer only; * denotes cleavage by both enantiomers. The relative intensity of alkylation and cleavage is represented by the number of symbols above a given site. The SV40 DNA numbering system employs the origin of replication (ORI) as a reference. Two regions of the SV40 DNA are represented. One region spans nucleotide no. 5189-138 and includes the origin of replication and part of the regulatory region. The other includes a segment of the SV40 early genes. The missing terminal regions of the SV40 DNA represented by a line constitute the nonoverlapping regions absent in the complementary clones and are not single-stranded segments of DNA. The data derived from c1346 are not shown.

the high affinity versus low affinity alkylation sites. A weak preference for the 3′ base preceding the alkylation site to be a purine base was detected, and this preference proved to be more characteristic of many of the low affinity versus high affinity alkylation sites. The alkylation selectivity for (+)-duocarmycin SA proved to be only subtly different from that of (+)-CC-1065, where the alkylation preference has been shown to be 5′-AAA$\underline{A}$ = 5′-TT$\underline{A}$ > 5′-AT$\underline{A}$, with a stronger preference for the fourth 5′ base to be A or T, an extended weak preference for the fifth 5′ base to be A or T, and the same weak preference for the 3′ base preceding the alkylation site to be a purine base.[28] Some of these distinctions are apparent from the data compiled in Table 2 which highlight the composite characteristics of the alkylation sites. Characteristic of the subtle differences between the duocarmycins and CC-1065 that do not readily appear in such a statistical analysis, (+)-CC-1065 fails to alkylate the minor 5′-CAA$\underline{A}$G site within w794 DNA as a consequence of its extended AT-rich binding selectivity (5 versus 3.5 base-pair binding site size) and more prominently alkylates the minor 5′-ATTT$\underline{A}$ and 5′-TTTT$\underline{A}$ sites which accommodate this extended five base-pair AT-rich binding site size, Figure 1. Like observations made in preceding studies,[8] the *seco*-(+)-duocarmycin SA agent **5** exhibited a DNA alkylation selectivity and efficiency identical with those of (+)-

Table 2. Summary of DNA Alkylation Sites

base[a,b]	−3	−2	−1	A	1	2	3	3′
			(+)-Duocarmycin SA [(+)-Duocarmycin A]					
A (30)	57 [59]	67 [57]	71 [74]	100	[45] 51	[37] 46	[41] 29	
T (26)	22 [18]	33 [35]	29 [24]		[18] 18	[24] 23	[18] 22	
G (21)	14 [10]	0 [2]	0 [0]		[31] 20	[26] 19	[18] 25	
C (23)	8 [12]	0 [6]	0 [2]		[6] 11	[12] 12	[22] 24	
A/T (56)	79 [77]	100 [92]	100 [98]	100	[63] 69	[61] 69	[59] 51	
Pu (51)					[76] 71			
Py (49)					[24] 29			
composite	A/T > G/C	A/T	A/T	A	Pu > Py	N	N	
base[a,b]	−3	−2	−1	A	1	2	3	3′
			(−)-Duocarmycin SA					
A (30)	46	52	70	100	77	53	35	
T (26)	21	23	23		19	20	21	
G (21)	16	11	0		0	17	26	
C (23)	17	14	7		4	10	18	
A/T (56)	67	75[c]	93	100	96[d]	73[d]	56	
Pu (51)								
Py (49)								
composite	N	N[e]	A/T	A	A/T	A/T > G/C	N	
base[a,b]	−4	−3	−2	−1	A	1	2	3	4	3′
				(+)-CC-1065						
A (30)	56	58	56	67	100	33	44	36	30	
T (26)	11	18	38	31		30	22	22	31	
G (21)	24	13	2	0		24	20	18	17	
C (23)	9	11	4	2		13	13	24	22	
A/T (56)	67	76	94	98	100	63	66	58	61	
Pu (51)						57				
Py (49)						43				
composite	A/T ≥ G/C	A/T > G/C	A/T	A/T	A	Pu > Py	N	N	N	
base[a,b]	−4	−3	−2	−1	A	1	2	3	4	3′
				(+)- and (−)-*N*-BOC-DSA						
A (30)				72	100	53				
T (26)				23		12				
G (21)				0		21				
C (23)				5		14				
A/T (56)				95	100	65				
Pu (51)						74				
Py (49)						26				
composite				A > T	A	Pu > Py				

[a] Percentage of the indicated base located at the designated position relative to the adenine N3 alkylation site. [b] The number in parentheses is the percentage composition within the DNA examined. [c] Potentially overestimated and attributable to minor alkylations derived from contaminate natural enantiomer (<0.1%), see text. [d] Potentially underestimated due to inclusion of minor sites derived from alkylations of contaminate natural enantiomer (< 0.1%), see text. [e] Taken from data derived from the high affinity or unique unnatural enantiomer sites.

duocarmycin SA itself, and the two agents were indistinguishable in our assays (4 or 25 °C, 24 h).

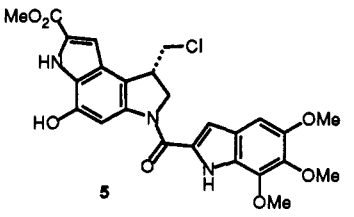

5

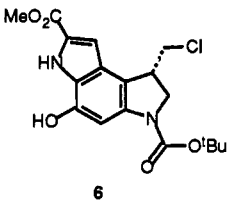

6

Quantitation, Isolation, and Characterization of the (+)-Duocarmycin SA–Adenine Adduct. The initial studies established that (+)-duocarmycin SA alkylated adenine within the minor groove in a manner comparable to (+)-duocarmycin A. The thermal cleavage of DNA used to identify the alkylation sites only detects adducts susceptible to thermal glycosidic bond cleavage (adenine N3, guanine N3, or guanine N7 alkylation), and potential alkylation events involving other nucleophilic centers in DNA (guanine C2-NH_2, thymine C2-O) may not be detected under such conditions. Consequently, quantitation of the adenine N3 alkylation reaction and confirmation of the structure of the product of the reaction were conducted through isolation and characterization of the thermally released adenine adduct.

This was addressed in a study of the alkylation of calf thymus DNA. Optimized conditions for calf thymus DNA (type I, Sigma)[38] alkylation were established for (+)-**1** on an analytical scale (100 μg of agent). For this purpose, the long-wavelength UV absorption of the agent and the adduct outside the UV absorption range of DNA provided a useful quantitative measure of the amount of adenine alkylation through UV quantitation of DNA bound (+)-**1**, quantitation of thermally released adduct **4**, and independent quantitation of recovered (+)-**1**. The preparative isolation of the adduct **4** was carried out under conditions determined to provide complete consumption of the agent. Thus, precipitation (EtOH) or extraction (EtOAc) of the calf thymus DNA following alkylation (25 °C, 24 h, 70 bp equiv DNA) afforded no recovered **1** (0%, UV quantitation) from the EtOH or EtOAc supernatant. Slightly higher yields of recovered **4** were obtained using the EtOAc extraction versus EtOH precipitation to remove unreacted agent. Thermal treatment of the alkylated DNA in aqueous 10 mM sodium phosphate buffer (100 °C, 25 min, pH 7.0) followed by EtOAc or *n*-BuOH extraction provided crude **4** in an exceptionally clean reaction. Although this thermolysis–extraction procedure was conducted a total of

(38) The calf thymus DNA was sonicated for 1 h and allowed to stand overnight to effect complete dissolution.

Table 3. ^{1}H NMR of **4** and N^3-Methyladenine (400 MHz) in Various Solvents[a]

	Compound **4**			
assignment	DMSO-d_6[b,c]	DMF-d_7[d]	CD_3OD, [CD_3OD–1% CF_3CO_2D[b]]	acetone-d_6[e]
N1-H (1H, s)[f]	11.70 [11.72]	[11.93]		10.73
N1′-H (1H, s)[f]	11.31 [11.31]	[11.28]		10.16
C6-OH (1H, s)	9.90 [9.92]	[10.28]		
NH_2 (2H, br s)	8.10 [9.25 (1H, br s)] [8.94 (1H, br s)]	[9.88] [9.26]		
Ade-C8-H (1H, s)	8.23 [8.55]	[8.70]	7.79 [8.20]	7.98
Ade-C2-H (1H, s)	7.95 [8.46]	[8.66]	7.40 [7.73]	8.12
C7-H (1H, br s)	7.76 [7.71]	[7.88]	7.55 [7.50]	7.92
C9′-H (1H, s)	6.88 [6.88]	[6.96]	6.93 [6.94]	6.89
C3′-H (1H, s)[f]	6.88 [6.88]	[7.04]	6.88 [6.89]	6.97
C3-H (1H, s)[f]	6.90 [6.75]	[6.90]	6.25 [6.68]	6.97
C13-H (1H)	4.66 [4.71] (dd, J = 13.6, 5.4 Hz)	[4.93] (dd, J = 13.6, 5.2 Hz)	4.67 [4.70] (dd, J = 13.9, 5.5 Hz)	4.89 (dd, J = 13.6, 4.9 Hz)
C13-H (1H)	4.47 [4.60] (dd, J = 13.6, 8.0 Hz)	[4.80] (dd, J = 13.6, 8.2 Hz)	4.59 [4.85] (obscured by CD_3OD)	4.67 (dd, J = 13.6, 7.4 Hz)
C11-H (1H)	4.48 [4.52] (br d, J = 11 Hz)	[4.74] (br d, J = 11.5 Hz)	4.66 [4.73] (br d, J = 11.6 Hz)	4.82 (br d, J = 11.0 Hz)
C11-H (1H)	4.49 [4.47] (dd, J = 11, 10 Hz)	[4.70] (dd, J = 11.5, 10 Hz)	4.60 [4.59] (dd, J = 11.2, 8.3 Hz)	4.61 (dd, J = 11.0, 8.6 Hz)
C10-H (1H, m)	4.33 [4.24]	[4.48]	4.23 [4.22]	4.55
C11′-OMe (3H, s)	3.91 [3.92]	[4.02]	4.04 [4.05]	4.02
C15-OMe (3H, s)	3.86 [3.86]	[3.94]	3.89 [3.92]	3.89
C13′-OMe (3H, s)	3.79 [3.80]	[3.88]	3.89 [3.89]	3.85
C12′-OMe (3H, s)	3.78 [3.78]	[3.87]	3.88 [3.88]	3.85

	N^3-Methyladenine		
assignment	DMSO-d_6[b,c]	CD_3OD	acetone-d_6[e]
N9- or N7-H (1H, br s)	[14.62]		
C6-NH_2 (2H)	7.79 [9.20 (s, 1H)] [9.17 (s, 1H)]		
Ade-C8-H (1H, s)	8.28 [8.72]	8.23 [8.56]	8.22
Ade-C2-H (1H, s)	7.74 [8.65]	7.89 [8.47]	7.79
N3-CH_3 (3H, s)	3.88 [3.97]	3.97 [4.07]	3.99

[a] The values for the protonated form of **4** or N^3-methyladenine are listed in brackets. Unless indicated otherwise, the coupling constants are derived from the ^{1}H NMR spectrum of protonated **4**. [b] Assignments based on 2D ^{1}H–^{1}H NOESY spectrum (400 MHz). [c] Assignments based on homonuclear decoupling. [d] Assignments based on the comparison of coupling constants derived from the spectrum in DMSO-d_6. [e] Assignments based on 2D ^{1}H–^{1}H ROESY spectrum (500 MHz). [f] Occasionally appears as a doublet, J = 1.8–2.2 Hz.

two times for each sample of alkylated DNA examined, the second thermal treatment provided little or no additional adduct **4**. The only UV active material detected in the organic extract proved to be **4**, and its extraction with EtOAc versus *n*-BuOH[9] proved equally effective but technically more convenient. The crude adduct **4** was purified by chromatography (SiO_2 deactivated with 5% Et_3N–CH_2Cl_2, 0–10% CH_3OH–CH_2Cl_2 eluent, 90–100% yield). Thus, the adenine N3 alkylation by (+)-duocarmycin SA was found to account for 90–100% of the consumption of the agent in the presence of duplex DNA and constitutes the predominant and near exclusive alkylation event under the conditions examined. As detailed in subsequent studies, the optimized conditions for stoichiometric thermal depurination versus reversal of the alkylation reaction employed low to neutral pH (7.0), rapid thermolysis at high temperature (100 °C), and low salt concentration (10 mM NaH_2PO_4–Na_2HPO_4). Each of these reaction parameters minimized deprotonation of the covalent adduct and enhanced denaturization of the duplex DNA, leading to quantitative thermal depurination. No (+)-duocarmycin SA derived from reversal of the alkylation reaction was detected (UV, TLC) in the thermal depurination reaction conducted under the conditions detailed.

The full physical and spectroscopic characterization of the adduct isolated as the free base led to the unambiguous assignment of the structure **4**. The ^{1}H NMR (Table 3 and Figure 3), 2D ^{1}H–^{1}H NOESY NMR, and ^{13}C NMR (Table 4) spectra of **4** and protonated **4** along with the comparison spectroscopic properties of N^3-methyladenine, the adenine–duocarmycin A adduct **7**,[8,9] *seco*-duocarmycin A[1–6] and SA (**5** and **6**)[21] agents, and related adenine N3 adducts[24,39,40] established adduct formation with

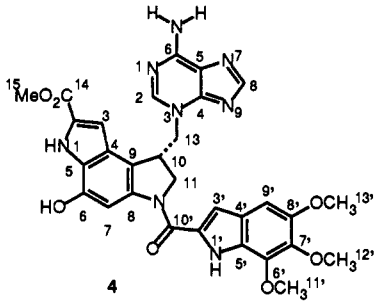

4

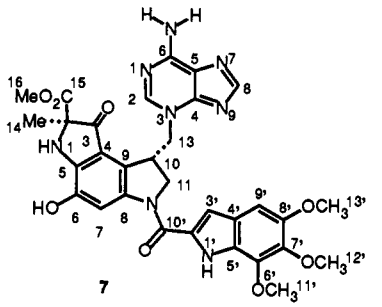

7

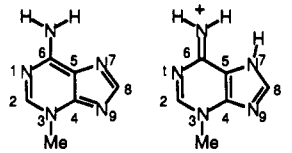

N^3-Me adenine

protonated N^3-Me adenine

adenine N3 addition to the unsubstituted cyclopropane carbon of **1**. In the ^{1}H NMR, the C10-H of adduct **4** was observed as a single proton (1H) at a characteristic chemical shift of 4.2–4.55 ppm. The C10-H NMR signal for the benzylic center resulting from alternative adenine N3 addition to the more

(39) Baker, B. F.; Dervan, P. B. *J. Am. Chem. Soc.* **1989**, *111*, 2700.

(40) Glusenkamp, K.-H.; Kruger, K.; Eberle, G.; Drosdziok, W.; Jahde, E.; Grundel, O.; Neuhaus, A.; Boese, R.; Stellberg, P.; Rajewsky, M. E. *Angew. Chem., Int. Ed. Engl.* **1993**, *32*, 1640. Yang, N.-C. C.; Chang, C.-W. *Proc. Natl. Acad. Sci. U.S.A.* **1985**, *82*, 5250. Calculated relative energies of the N7-H, N9-H, and NH_3^+ tautomers for protonated N^3-methyladenine are 0.0, 2.2, and 26.7 kcal/mol (AM1) and 0.0, 4.9, and 24.8 kcal/mol (MNDO), respectively.

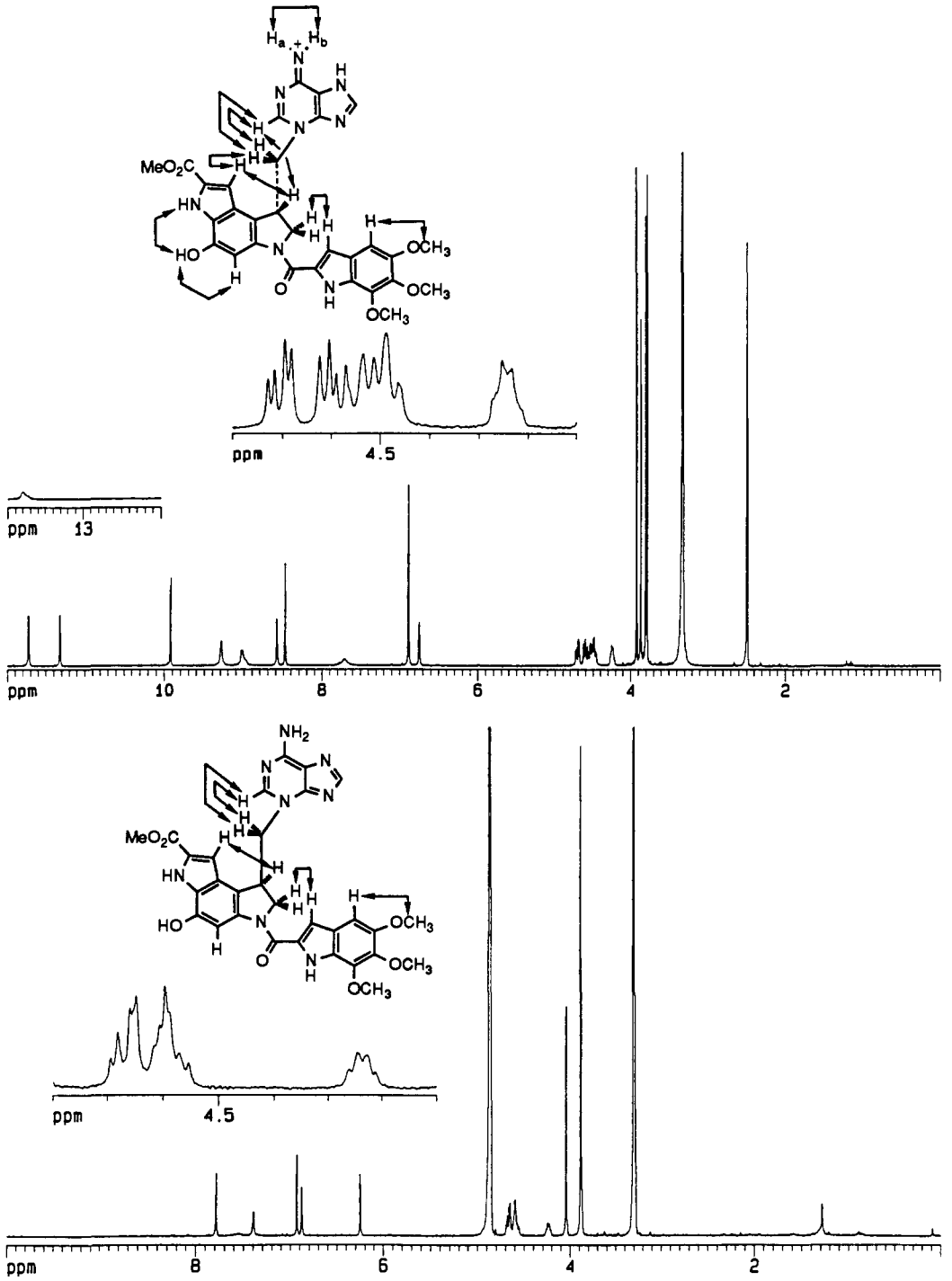

Figure 3. (Top) ^{1}H NMR (DMSO-d_6, 400 MHz) of protonated (+)-**4** and structure illustrating the diagnostic ^{1}H–^{1}H NOEs. (Bottom) ^{1}H NMR (CD_3OD, 400 MHz) of (–)-**4** and structure illustrating the diagnostic ^{1}H–^{1}H NOEs.

substituted cyclopropane carbon would appear as two protons (3.5–3.6 ppm, 2H) with a large geminal coupling constant (J = 19.5 Hz) characteristic of duocarmycin B_1/C_1.[2] The additional chemical shifts of C11-H (2H) and C13-H (2H), their observed couplings, and the assigned coupling constants were fully consistent with this assignment. Characteristic of an adenine N3 alkylation product, the adenine C2-H and C8-H (1H each) were readily distinguishable[40] and the two exchangable protons appeared as a broadened singlet (2H, C6-NH_2). Although two tautomeric forms of the N3-alkylated adenine are possible, **4** with two amine protons at N6 or a structure with one proton at N6 and a second proton at N7/N9, the former has been assigned to **4** on the basis of this equivalency of the two exchangeable protons and in analogy with past studies based on a careful analysis of the ^{15}N NMR of a closely related bromoacetyldistamycin C6-N^{15} adenine N3 adduct.[39] Interestingly, two broad singlets of one proton each for protonated **4** were observed in DMSO-d_6 (Figure 3, 9.25 and 8.94 ppm) and DMF-d_7 for the C6-NH_2 protons. The chemical shift of the nonequivalent C6-NH_2 protons proved to be somewhat concentration dependent, and at lower concentrations the two signals broadened but the two signals did not coalesce, even at 1 mM. This clearly illustrates that the protonated adduct, like protonated N^3-methyladenine itself, suffers restricted rotation about the C6-NH_2 bond consistent with the tautomeric form depicted in Table 3 and Figure 3 bearing a $^6C{=}NH_2^+$. The remaining exchangeable proton of protonated **4** and protonated N^3-methyladenine resides at N7 or N9, and while we were not able to experimentally distinguish between the two possibilities, the N7-H tautomeric form would be expected to be more stable.[40]

The ^{13}C NMR of **4** was found to be in excellent agreement with that of the adenine–duocarmycin A adduct **7**[9] (Table 4) and diagnostic of adenine N3 addition to the unsubstituted cyclo-

Table 4. ^{13}C NMR of **4** (100 MHz) and Related Agents in Various Solvents

4[a]			7		1	
assignment	DMSO-d_6	acetone-d_6	assignment	CD_3OD	assignment	acetone-d_6
C-2	125.6	126.9	C-2	72.0	C-2	131.0
C-3	105.6	106.2	C-3	199.4	C-3	108.9
C-4	124.1	125.5	C-4	119.2	C-4	127.2
C-5	128.0	129.3	C-5	145.8	C-5	132.9
C-6	145.0	145.0	C-6	140.3	C-6	178.0
C-7	112.6	113.3	C-7	112.7	C-7	112.5
C-8	138.0	139.7	C-8	138.2	C-8	161.6
C-9	100.3	102.0	C-9	116.1	C-9	31.9
C-10	~40.0[b]	41.1	C-10	41.2	C-10	26.4
C-11	52.4	53.9	C-11	54.1	C-11	55.8
C-13	57.8	58.9	C-13	59.9	C-13	24.5
C-2′	131.4	132.0	C-2′	131.4	C-2′	130.6
C-3′	105.8	106.7	C-3′	108.0	C-3′	108.4
C-4′	123.2	124.7	C-4′	125.1	C-4′	124.4
C-5′	125.0	126.2	C-5′	127.1	C-5′	127.6
C-6′	139.0	140.0	C-6′	140.3	C-6′	140.0
C-7′	139.6	141.2	C-7′	141.6	C-7′	141.9
C-8′	149.5	149.9	C-8′	149.0	C-8′	151.2
C-9′	97.9	98.9	C-9′	99.5	C-9′	98.9
C-10′	159.6	160.3	C-10′	161.2	C-10′	162.0
C-11′	55.9	56.5	C-11′	56.6	C-11′	56.4
C-12′	61.1	61.5	C-12′	62.0	C-12′	61.5
C-13′	60.9	61.4	C-13′	61.8	C-13′	61.4
			C-14	23.6		
C-14	161.3	162.4	C-15	170.6	C-14	162.4
C-15	51.8	52.1	C-16	53.4	C-15	51.9
Ade-C2	151.5	153.0	Ade-C2	152.4		
Ade-C4	149.5	149.9	Ade-C4	151.0		
Ade-C5	123.7	122.7	Ade-C5	122.3		
Ade-C6	154.8	155.6	Ade-C6	155.5		
Ade-C8	145.0	146.4	Ade-C8	148.0		

assignment	CD_3OD	CD_3OD + 2% CF_3CO_2D	DMSO-d_6	DMSO-d_6 + 1% CF_3CO_2D	DMF-d_7
			N^3-Methyladenine		
Ade-C2	152.9	149.7	152.4	148.5	153.6
Ade-C4	151.1	150.0	150.3	148.3	150.6
Ade-C5	120.8	111.9	120.3	110.4	120.3
Ade-C6	156.8	155.4	154.9	153.5	155.6
Ade-C8	146.0	146.1	143.9	145.2	146.2
N3-CH_3	36.9	36.8	35.8	36.1	36.0

[a] Free base of **4**. [b] Obscured by DMSO.

propane carbon. The key signals distinguishing the possible adducts are found in the carbons within or proximal to the fused five- versus six-membered ring with **4** exhibiting chemical shifts consistent only with the former, *i.e.*, C10 at 40–41 ppm consistent with duocarmycin B_2/C_2 (41–43 ppm),[1-6] *seco-N*-BOC-DSA (**6**, 42.6 ppm),[21] and **7** (41.2 ppm)[9] versus 33–34 ppm for duocarmycin B_1/C_1. Similarly, the C8 signal for **4** was observed at 138–139 ppm consistent with duocarmycin B_2/C_2 (138–137 ppm) and **7** (138.2) versus 128–129 ppm for duocarmycin B_1/C_1, and the C7 singlet was observed at 112–113 ppm also consistent with duocarmycin B_2/C_2 (112–113 ppm) and **7** (112.7) versus 117–118 ppm for duocarmycin B_1/C_1.

The structure of **4** and the ^1H NMR assignments were firmly established through interpretation of the 2D ^1H–^1H NOESY NMR (DMSO-d_6, CD_3OD) or 2D ^1H–^1H ROESY NMR (acetone-d_6), which proved consistent only with the structure **4**. The diagnostic NOEs observed in DMSO-d_6 are illustrated in Figure 3 and summarized in the Experimental Section. The observed NOEs in DMSO-d_6, along with those observed in CD_3OD and acetone-d_6, served to unambiguously establish the N1-H, C3-H, C6-OH, C7-H, C10-H, C11-H_a and -H_b, C13-H_2, Ade-C2-H, Ade-C8-H, C3′-H, C9′-H, and C8′-OCH_3 assignments, and the lack of a detectable diagnostic Ade-C2-H/C11-H_2 NOE rules out the alternative adduct structure derived from adenine addition to the more substituted cyclopropane carbon of **1**.

Thus, the isolation, quantitation, and full characterization of the thermal depurination product confirmed the assignment of the structure **4** and unambiguously established the predominant (+)-duocarmycin SA DNA alkylation reaction (90–100%) as that which proceeds by adenine N3 addition to the unsubstituted cyclopropane carbon.

Reversibility of the Duocarmycin SA and Duocarmycin A DNA Alkylation Reaction. Although the nature of the (+)-duocarmycin SA and (+)-duocarmycin A DNA alkylations has proven similar to that of (+)-CC-1065, one important feature of the reactions distinguish the two classes of natural products. Unlike (+)-CC-1065, which essentially irreversibly alkylates duplex DNA,[41] (+)-duocarmycin SA and (+)-duocarmycin A, like simplified analogs of CC-1065,[41] were found to reversibly alkylate DNA. The relative rate or ease of reversibility proved dependent upon the relative reactivity of the agent and hence the stability of the adduct as well as the extent of the agent noncovalent binding interactions.

The reversible nature of the duocarmycin A or SA DNA alkylation reaction was monitored through measurement of the transfer of agent from unlabeled duplex DNA covalently modified with **1** or **3** to unmodified radiolabeled w794 duplex DNA. The detection of the agent transfer reaction and the identification of the sites of labeled w794 DNA alkylation were established following the procedure in which thermolysis (100 °C, 30 min) of the covalently modified DNA induces stand cleavage at the adenine N3 alkylation sites.

Unlabeled duplex w794 DNA was treated with (+)-**1** or (+)-**3** under conditions which ensure complete alkylation (1–7 days, 4–25 °C). Under these conditions, complete alkylation generally required less than 24 h, but the extended reaction times ensured complete reaction. Unbound agent was removed using an extensive extraction procedure consisting of sequential phenol extraction (1×), BuOH extraction (2×), and Et_2O extraction (1×) followed by EtOH precipitation and isolation of the duplex DNA. This extensive extraction and precipitation procedure ensured that no unbound or noncovalently bound agent remained in the sample of unlabeled duplex DNA. As illustrated in Figures 4 and 5, this expectation was further supported by the observation that the transfer of agent from the unlabeled to labeled DNA was found to occur slowly and linearly over a period of >4–8 days (50 °C), whereas the alkylation of duplex DNA by free agent is complete after 12–24 h (25 °C). Following removal of the EtOH supernatant, the covalently modified unlabeled duplex DNA was redissolved in aqueous buffer, mixed with ^{32}P singly 5′ end-labeled w794 DNA at concentrations which represent 4:1, 1:1, and 0.5:1 molar ratios of unlabeled:labeled w794 DNA, and incubated at 4–50 °C under a variety of reaction conditions for 8, 4, 2, and 1 days. Thermolysis (100 °C, 30 min), high-resolution PAGE, autoradiography, and quantitation of intact labeled DNA and the cleavage bands permitted detection of the alkylation of labeled w794 DNA, quantitation of the transferred agent constituting a measure of the reversible DNA reaction, and identification of the sites of labeled w794 DNA alkylation. The extent of the transfer of the agent and hence the reversibility of the DNA alkylation reaction proved sensitive to the reaction conditions. Increasing the pH (8.4 > 7.4 > 6.0), temperature (50 °C > 37 °C > 25 °C > 4 °C), time (8 days > 4 days > 2 days > 1 day) and, to a lesser extent, the salt concentration (200 mM NaCl ≅ 100 mM > 50 mM) led to increased transfer of agent from unlabeled to labeled duplex DNA. At higher pH, deprotonation of the phenol adduct presumably accounts for the acceleration of retroalkylation, while high salt concentration stabilizes duplex versus denatured DNA and diminishes the extent of competitive thermal depurination. This latter competitive reaction occurs more readily within denatured DNA and is only important at the higher reaction temperatures where depurination is observed. Two sites were alkylated within the 144 base-pairs of the labeled duplex w794 DNA and constitute the major, high affinity (5′-

(41) Warpehoski, M. A.; Harper, D. E.; Mitchell, M. A.; Monroe, T. J. *Biochemistry* **1992**, *31*, 2502. For related studies, see: Lee, C.-S.; Gibson, N. W. *Biochemistry* **1993**, *32*, 9108.

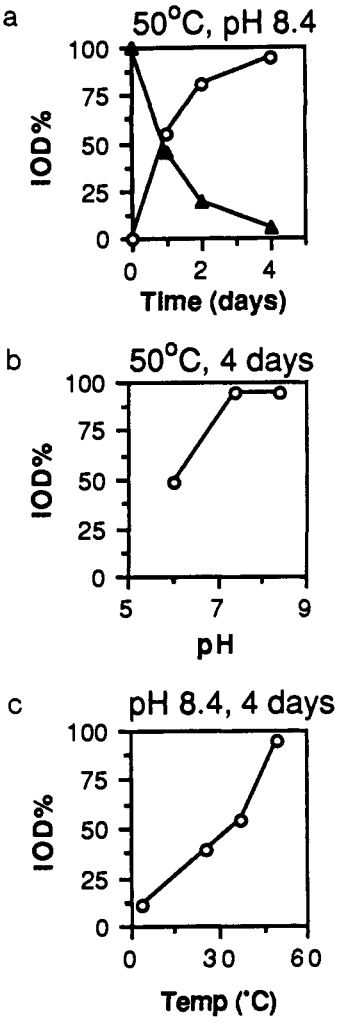

Figure 4. Time, pH, and temperature dependence of the reversible (+)-duocarmycin SA (**1**) DNA alkylation reactions. The time (a), pH (b), and temperature (c) dependences were determined by incubation of 5′ end-labeled SV40 DNA (clone w794/w836) with **1**-covalently modified unlabeled w794/w836 DNA (1:4 molar ratio) followed by thermally-induced cleavage (100 °C, 30 min), 8% denaturing PAGE, and autoradiography. Integrated optical density (IOD) was determined for the unmodified labeled DNA, the high affinity alkylation site cleavage band, and the low affinity alkylation site cleavage band on a BioImage Model 60S RFLP system. ▲, unmodified labeled DNA; O, high affinity alkylation/cleavage sites.

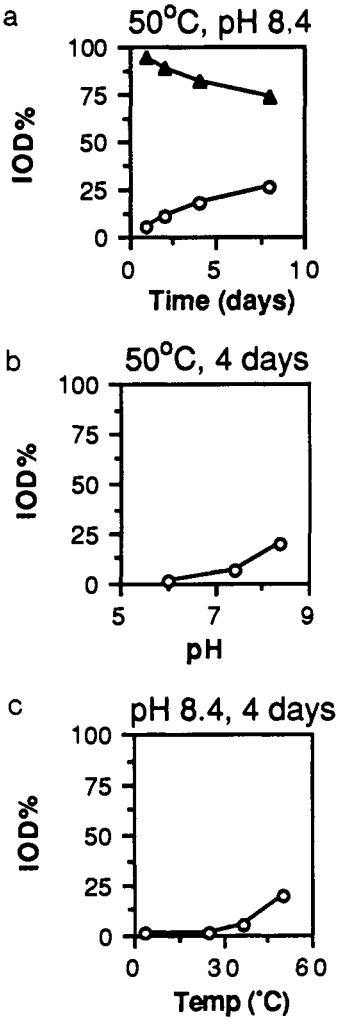

Figure 5. Time, pH, and temperature dependence of the reversible (+)-duocarmycin A (**3**) DNA alkylation reactions. The time (a), pH (b), and temperature (c) dependences were determined by incubation of 5′ end-labeled SV40 DNA (clone w794/w836) with **3**-covalently modified unlabeled w794/w836 DNA (1:4 molar ratio) followed by thermally-induced cleavage (100 °C, 30 min), 8% denaturing PAGE, and autoradiography. Integrated optical density (IOD) was determined for the unmodified labeled DNA, the high affinity alkylation site cleavage band, and the low affinity alkylation site cleavage band on a BioImage Model 60S RFLP system. ▲, unmodified labeled DNA; O, high affinity alkylation/cleavage sites.

AATTA) and minor, low affinity (5′-CAAAG) sites. The quantitation of the transfer of the agents to these two sites is presented in Figures 4 and 5.

The ramifications of these observations are especially significant. First, the relative ease or rate of reversibility proved greatest with (+)-duocarmycin SA. At a 4:1 molar ratio of unlabeled:labeled DNA, the reversal of the (+)-duocarmycin SA alkylation resulted in complete consumption of the labeled DNA within 4 days (50 °C) at pH 8.4 and 7.4. At pH 8.4, the reversal of the (+)-duocarmycin SA DNA alkylation was detectable even at 4 °C, proved effective at temperatures of 25 and 37 °C, and led to complete consumption of the labeled DNA at 50 °C (4 days). At 50 °C (4 days), the reversal of the (+)-duocarmycin SA alkylation led to complete consumption of the labeled DNA at pH 8.4 and 7.4, and detectable but substantially diminished consumption was seen at pH 6.0. In contrast, the reversal of the (+)-duocarmycin A alkylation reaction proved much slower. After 8 days (pH 8.4, 50 °C), only 25% of the labeled DNA was consumed by released agent, detectable but substantially diminished reversibility was observed at pH 7.4, and little or no released agent was detected at pH 6.0. Even at pH 8.4, no released (+)-duocarmycin A was detected at 4 or 25 °C, detectable released agent was observed at 37 °C, and only at 50 °C did the reversibility of the alkylation become easily detectable. Thus, consistent with the relative reactivity of the agents (A > SA)[21] and hence the expected stability of the adducts, the (+)-duocarmycin A retroalkylation reaction proved much slower and less effective than that of (+)-duocarmycin SA under all conditions examined. In addition, (+)-CC-1065 possesses an inherent reactivity which is less than that of (+)-duocarmycin A but greater than that of (+)-duocarmycin SA.[21] The lack of detection of a reversible (+)-CC-1065 DNA alkylation reaction[41] suggests that the extent or rate of reversibility is additionally dependent upon the extent of the noncovalent binding stabilization of the agent. Consistent with this interpretation, *N*-BOC-CPI and simplified analogs of CC-1065 possessing the natural CPI alkylation subunit embodying structures which provide less noncovalent binding stabilization do reversibly alkylate duplex DNA.[41] In the course of early studies on (+)-CC-1065 and their more recent extension to the duocarmycins, extensive computational and quantitative molecular modeling studies in conjunction with an intuitive appreciation of the chemical properties of the agents led us to propose that the adenine N3 alkylation reaction could be expected to represent a reversible, near thermal neutral reaction stabilized by extensive

noncovalent binding interactions.[11,23,28] The fact that the duocarmycin SA and CC-1065 adenine N3 addition reaction is not observed with free adenine external to duplex DNA further suggests that the dominant forces driving the DNA alkylation reaction are not the covalent bonding forces but rather the noncovalent binding stabilization derived from hydrophobic binding and van der Waals contacts,[19] a process we continue to refer to as hydrophobic binding-driven-bonding.[11,23] That is, the near thermal neutral and inherent reversible nature of the alkylation reaction is rendered less reversible or irreversible by dominant stabilizing noncovalent binding interactions.

The relevance of these proposals has become important in the comparison of the biological properties of the agents. Like the comparisons of (+)-CC-1065, (+)-CPI-PDE_1 and (+)-CPI-$CDPI_n$ (n = 1–3) with (+)-*N*-BOC-CPI,[28] the exceptionally potent cytotoxic activity of (+)-duocarmycin SA (**1**; 10 pM, L1210) versus the relative nonpotent activity of (+)-*N*-BOC-DSA (**2**; 6 nM, L1210) may be attributed to the simple event of noncovalent binding stabilization of the inherently reversible DNA alkylation reaction.[21] The demonstration of the slow, reversible nature of the duocarmycin DNA alkylation reaction, the establishment of the reversible CPI DNA alkylation reaction,[41] and the dependence of the degree of reversibility on the relative reactivity of the agent as well as the extent of the noncovalent binding affinity suggest this feature of the agents' behavior may play a fundamental role in the expression of their biological properties.

We have also suggested that the extent of the noncovalent binding stabilization may be directly related to the unique and characteristic fatal, delayed toxicity of (+)-CC-1065 and (+)-CPI-$CDPI_2$ which is not embodied in its simpler analogs or in duocarmycin A and SA. As we have suggested elsewhere,[12] the delayed toxicity of (+)-CC-1065 may be the consequence of the extent of the noncovalent binding stabilization which renders the DNA alkylation reaction essentially irreversible.

Model of the (+)-Duocarmycin SA DNA Alkylation. The unambiguous structural characterization of the adenine–duocarmycin SA adduct establishing adenine N3 addition to the unsubstituted cyclopropane carbon, the established absolute configuration of the agents,[6] and the identification of the sequence preference for minor groove alkylation that clearly extends in the 5′ direction from the site of adenine alkylation permit the construction of an accurate model of this predominant (+)-duocarmycin SA DNA alkylation event.

This is illustrated in Figure 6 with the comparison of (+)-duocarmycin SA and (+)-duocarmycin A[8] within the w794 DNA high affinity alkylation site. The bound helical conformations of the agents complement the topological curvature and pitch of the minor groove with agent binding spanning 3.5 base-pairs in the 5′ direction from the adenine N3 alkylation site. The hydrophobic concave face of the agent is deeply imbedded in the minor groove, and the polar functionality of the agent lies on the outer face of the complex. We attribute the alkylation selectivity in part to the noncovalent binding selectivity of the agent within the narrower, sterically more accessible AT-rich minor groove[19,32] and the 3.5 base-pair binding site size required to permit full agent binding. This nicely explains the observed absolute requirement for the first three base-pairs of the alkylation sites to be A or T that extends less rigidly to include the fourth base-pair.

Importantly, this interpretation should not be misconstrued to imply that AT-rich binding necessarily leads to productive DNA alkylation. Rather, the noncovalent binding of the agents may serve to further restrict the number of available alkylation sites. Additional distinctions in the facility or rate of DNA alkylation within the available binding sites will be expectedly observed due to steric accessibility to the alkylation center and stereoelectronic effects imposed on the alkylation reaction. A simple interpretation of the results to date suggests that the depth of minor groove penetration by the agent and steric accessibility to the alkylation site are important features contributing to the observed efficiency or intensity of DNA alkylation. As detailed in subsequent studies, for simple derivatives of the alkylation subunit, sufficient minor groove penetration is possible with a single 5′ A or T base adjacent to the alkylation site. For (+)-**1**, sufficient minor groove penetration may be possible only when two or more adjacent 5′ bases are A or T.

In addition to significantly enhancing the sequence selectivity of the DNA alkylation reaction, the trimethoxyindole subunit of (+)-**1** serves the further important functional role of stabilizing the inherently reversible nature of the adenine N3 alkylation reaction. We further suggest that the simple event of this noncovalent binding stabilization of the reversible DNA alkylation reaction is responsible for the potent biological activity of (+)-**1** versus (+)-**2**.

(+)-and (–)-*N*-BOC-DSA. The examination of the DNA alkylation properties of both enantiomers of *N*-BOC-DSA proved especially revealing. The *tert*-butyloxycarbonyl (BOC) derivative was selected for study since extensive comparative data were available for a series of structurally related agents including *N*-BOC-CPI (**8**),[28] *N*-BOC-CBI (**9**),[33] and *N*-BOC-CI (**10**).[32]

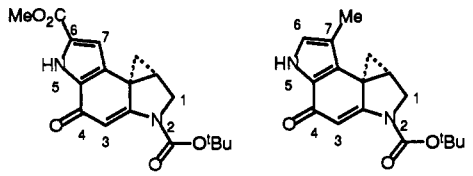

2 (+)-N-BOC-DSA **8** (+)-N-BOC-CPI

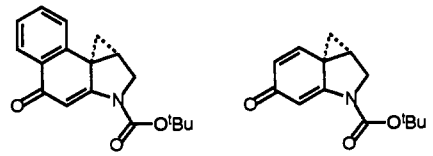

9 (+)-N-BOC-CBI **10** (+)-N-BOC-CI

As detailed elsewhere,[28] the choice of a simple derivative (BOC) may subtly affect the relative selectivity among the available alkylation sites and the efficiency of DNA alkylation, but it does *not* alter the sites of alkylation detected over a 10-fold concentration range. The DNA alkylation by the simple subunits proved substantially less selective than that of (+)- or (–)-duocarmycin SA. Within the five 150 base-pair segments of DNA examined, 40–45% of the adenines were alkylated by the agents within a 10-fold concentration range. This is in contrast to 20–25% alkylation of the total adenines available by (+)-duocarmycin SA over a 1000–10 000-fold concentration range. Contrary to some expectations but consistent with past observations, (+)-*N*-BOC-DSA and (–)-*N*-BOC-DSA displayed comparable, essentially identical DNA alkylation profiles. Both enantiomers of **2** were found to alkylate DNA only at concentrations approximately 10 000 times that required for (+)-duocarmycin SA and generally required more vigorous reaction conditions (37 °C, 24 h versus 4–25 °C, 24 h), Figure 7. Table 5 summarizes the alkylation sites for (+)- and *ent*-(–)-*N*-BOC-DSA observed over a 10-fold concentration range. In *all* cases, only strand cleavage derived from adenine N3 alkylation was observed, and no evidence for even a single guanine N3 alkylation was detected. In all but four instances of a 5′-C<u>A</u> alkylation, the adenine N3 alkylation was found to occur within a two base AT-rich site. The preference for DNA alkylation proved to be 5′-A<u>A</u> > 5′-T<u>A</u>, with the additional distinct preference for a purine base at the 3′ site preceding the alkylation site. The agents also appear to exhibit a weak preference for the third base to be A or T versus G or C, although this needs to be interpreted with caution since 40–45% of all adenines are reactive toward the agents over a small 10-fold concentration range. In addition, both enantiomers of the seco agent **6** proved indistinguishable from **2** in the DNA alkylation assays. At least part if not all of the origin of the 5′-A<u>A</u> > 5′-T<u>A</u>

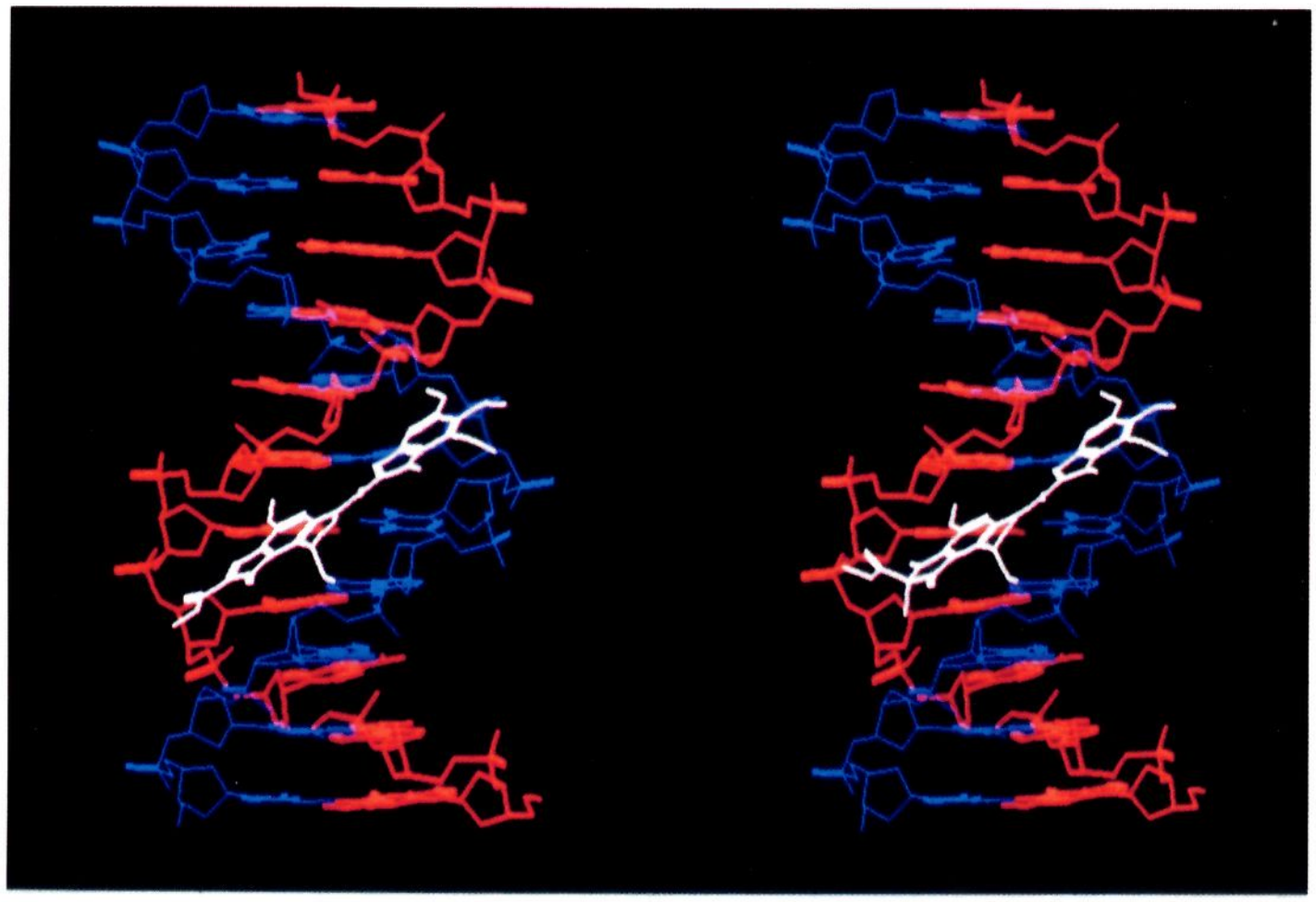

Figure 6. Comparison stick and space-filling models of (+)-duocarmycin SA and (+)-duocarmycin A within the high affinity alkylation site of w794 DNA: duplex 5′-d(CTCAATTAGTC). The model complexes were generated with MacroModel (AMBER force field supplemented with parameters for duocarmycin SA and A) and subjected to full complex minimization.

preference lies in the statistically relevant equal opportunity for alkylation of the unlabeled complementary strand adenine within the 5′-TA sites competitive with the labeled strand site. Since the occurrence of alkylation at 5′-TA is almost 50% that of 5′-AA alkylation, the observed preference may well be simply statistical and the result of competitive complementary strand alkylation within the 5′-TA sites that precludes additional labeled strand alkylation, lowering the apparent 5′-TA alkylation efficiency.

Two important distinctions between the DNA alkylation profiles of **2** and duocarmycin SA (**1**) deserve highlighting. Clear from the comparison within w794 DNA (Figure 7) are the more selective DNA alkylation properties of (+)-**1** or (−)-**1** versus that of (+)- or (−)-**2**. That is, (+)-**1** and (−)-**1** each alkylate a different subset of sites within the set of sites alkylated by (+)- or (−)-**2**. However, this simple description, while nearly accurate, is not entirely complete. There exists a small subset of sites that either (+)-duocarmycin SA or (−)-duocarmycin SA alkylates which are not alkylated by *N*-BOC-DSA. For (+)-duocarmycin SA, this subset characteristically contains the 5′-TTA sequence, which has proven to be a high affinity site for the natural agent and yet embodies the less preferred sequence for **2**, 5′-AA > 5′-TA. Characteristic of this distinction, (+)-duocarmycin SA alkylated 53% of all 5′-TTA sites while (+)- and (−)-*N*-BOC-DSA alkylated only 42%. In addition, many of the 5′-TTA sites alkylated by *N*-BOC-DSA were not alkylated by (+)-duocarmycin SA. As

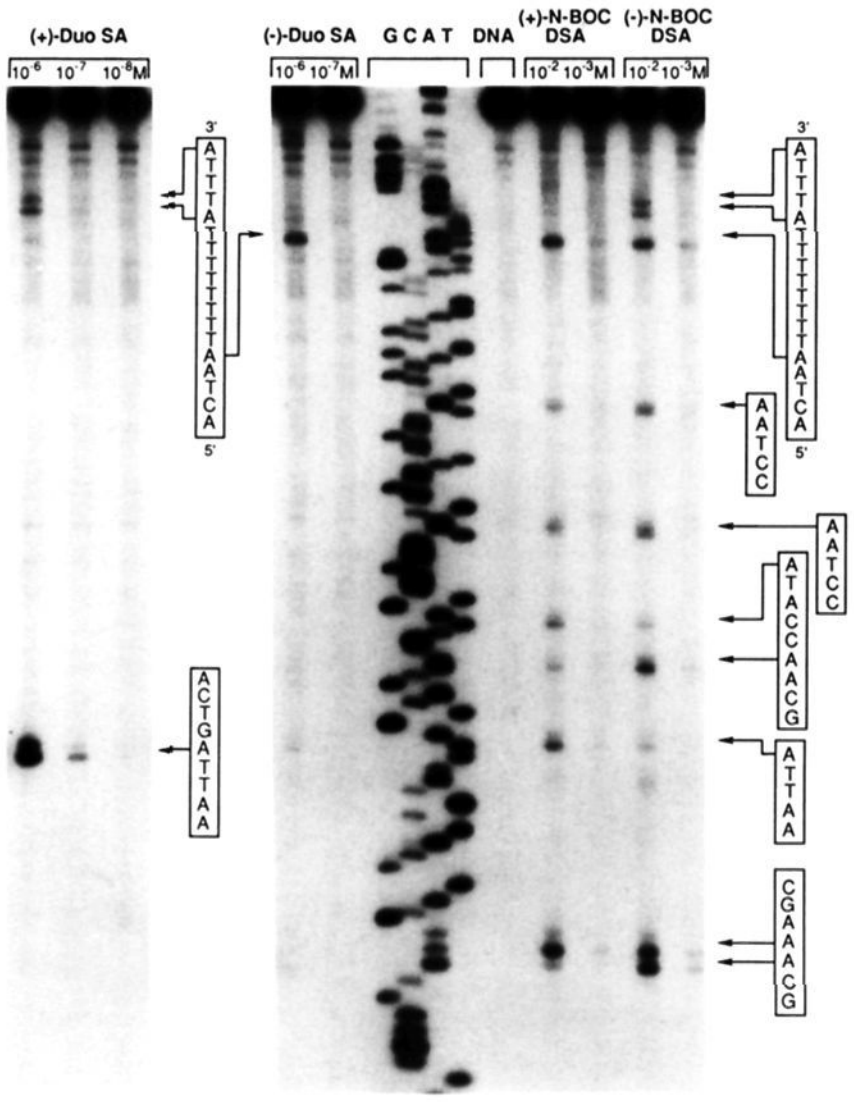

Figure 7. Thermally-induced strand cleavage of w794 DNA (SV40 DNA segment, 144 bp, nucleotide no. 138-5238). DNA–agent incubation at 25 °C (24 h) for (+)- and (–)-duocarmycin SA and at 37 °C (24 h) for (+)- and (–)-*N*-BOC-DSA, removal of unbound agent and 30 min thermolysis (100 °C), followed by denaturing 8% PAGE and autoradiography. Lanes 1–3, (+)-duocarmycin SA ((+)-**1**, 1×10^{-6} to 1×10^{-8} M); lanes 4–5, (–)-duocarmycin SA ((–)-**1**, 1×10^{-6} to 1×10^{-7} M); lanes 6–9, Sanger G, C, A, and T reactions; lane 10, control DNA; lanes 11–12, (+)-*N*-BOC-DSA ((+)-**2**, 1×10^{-2} to 1×10^{-3} M); lanes 13–14, (–)-*N*-BOC-DSA ((–)-**2**, 1×10^{-2} to 1×10^{-3} M).

Table 5. Summary of DNA Alkylation Sites for (+)- and (–)-*N*-BOC-DSA

sequence	no. total sites	no. alkylated sites
5′-(NAAN)-3′	83	62 (75%)
5′-(AAAN)-3′	39	33 (85%)
5′-(TAAN)-3′	19	17 (89%)
5′-(GAAN)-3′	11	3 (27%)
5′-(CAAN)-3′	14	9 (64%)
5′-(NAAPu)-3′	54	45 (83%)
5′-(NAAPy)-3′	29	17 (59%)
5′-(NTAN)-3′	53	21 (40%)
5′-(ATAN)-3′	18	11 (61%)
5′-(TTAN)-3′	19	8 (42%)
5′-(GTAN)-3′	7	2 (29%)
5′-(CTAN)-3′	9	0 (00%)
5′-(NTAPu)-3′	29	16 (55%)
5′-(NTAPy)-3′	24	5 (21%)

such, (+)-duocarmycin SA and (–)-duocarmycin SA are not only more selective among the available alkylation sites but also distinct in their alkylation profiles as well.

The concentration of (+)-*N*-BOC-DSA required for observation of DNA alkylation proved comparable but slightly lower than that required for DNA alkylation by *N*-BOC-CPI,[28] the alkylation subunit of (+)-CC-1065. This more efficient DNA alkylation reaction of (+)-*N*-BOC-DSA versus (+)-*N*-BOC-CPI (ca. 5 times more efficient) may be attributed in part to the enhanced stability of **2**, which leads to a more productive participation in the DNA alkylation reaction. However, this undoubtedly constitutes only part of the observed differences. The DSA-based agents participate in the DNA alkylation reaction at a rate that exceeds that of the more reactive CPI-based agents, and this contributes to the DNA alkylation intensity differences of (+)-*N*-BOC-DSA and (+)-*N*-BOC-CPI. As described in more detail later on, we believe this enhanced rate of DNA alkylation is derived from a decreased steric hindrance surrounding the DSA vs CPI C7 center.

In addition to the observation that both enantiomers of *N*-BOC-DSA alkylate DNA with essentially the same selectivity, we find that they do so with no apparent differences in efficiency. Similar observations have been made in the comparisons of (+)- and (–)-*N*-BOC-CI,[32] but they are distinct from the results of the comparisons of (+)- and (–)-*N*-BOC-CPI[28] or (+)- and (–)-*N*-BOC-CBI.[33] With the latter agents, the natural enantiomers proved to be 5–10 times more efficient at alkylating DNA and 5–10 times more cytotoxic than the corresponding unnatural enantiomers.[42] As described in more detail later on, we believe this diminished distinction between the pairs of enantiomers is the result of the decreased steric hindrance surrounding the DSA C7 center for which the unnatural enantiomers are especially sensitive.

In our comparison of the results derived from the evaluation of *N*-BOC-DSA (**2**), *N*-BOC-CPI (**8**),[28] *N*-BOC-CBI (**9**),[33] and *N*-BOC-CI (**10**),[32] it is clear that both enantiomers of all four classes of agents alkylate the same composite sites in duplex DNA. The distinction among the agents lies not in the number of sites alkylated over an agent 10-fold concentration range but in the efficiency of DNA alkylation and the relative selectivity among the available alkylation sites. Although the relative selectivity differences are subtle, the least reactive agents not only produce a more intense or efficient DNA alkylation (*N*-BOC-DSA and *N*-BOC-CBI > *N*-BOC-CPI > *N*-BOC-CI) but also do so with more discrimination among the available sites. While this unusual behavior of both enantiomers alkylating the same sites within DNA may appear unexpected, it does suggest that the event and selectivity of DNA alkylation is tied to the DNA versus agent structure. This prospect is further reinforced by the observation that the characteristic alkylation profile for the four classes of agents is not uniquely observed with agents containing the activated cyclopropane but other electrophiles incorporated into structurally related agents behave similarly.[8,31] Thus, in addition to being independent of the absolute configuration of the agents, the characteristic alkylation selectivity also appears to be independent of the nature of the electrophile within the limited series of agents examined to date.

The selectivity of DNA alkylation in past studies has been attributed to a sequence-dependent autocatalytic phosphate protonation of the alkylation subunit carbonyl,[22,27,43] the conformational variability of DNA and alkylation at junctions of bent DNA,[44] or alkylation within the narrower, sterically more accessible minor groove of AT-rich DNA.[10,11,28–33] Central to the distinctions in the interpretations have been the perceived similarities[27] or distinctions[28] in the alkylation selectivity of simple derivatives of the alkylation subunit versus the natural products themselves. Consistent with the latter interpretation of the origin of the alkylation selectivity, the most prevalent feature of the DNA alkylation sites is the neighboring 5′ base-pairs, Table 2. While this requirement for a single 5′ A or T base adjacent to the adenine alkylation site for both enantiomers of **2** may seem intuitively unlikely, constructed models of the diastereomeric alkylations proved revealing. For the natural enantiomer, this simply involves 3′ adenine N3 alkylation and agent binding in the 3′→5′ direction from the site of alkylation across the adjacent 5′ base, see Figures 6 and 8. For the unnatural enantiomer, this similarly requires adenine N3 alkylation but with the reversed

(42) This may prove consistent with the possibility that the relative biological potency of the enantiomeric agents or their apparent DNA alkylation efficiency is not related to the rate of DNA alkylation but rather to the relative stability of the adducts.

(43) Lin, C. H.; Beale, J. M.; Hurley, L. H. *Biochemistry* **1991**, *30*, 3597.
(44) Sun, D.; Lin, C. H.; Hurley, L. H. *Biochemistry* **1993**, *32*, 4487.

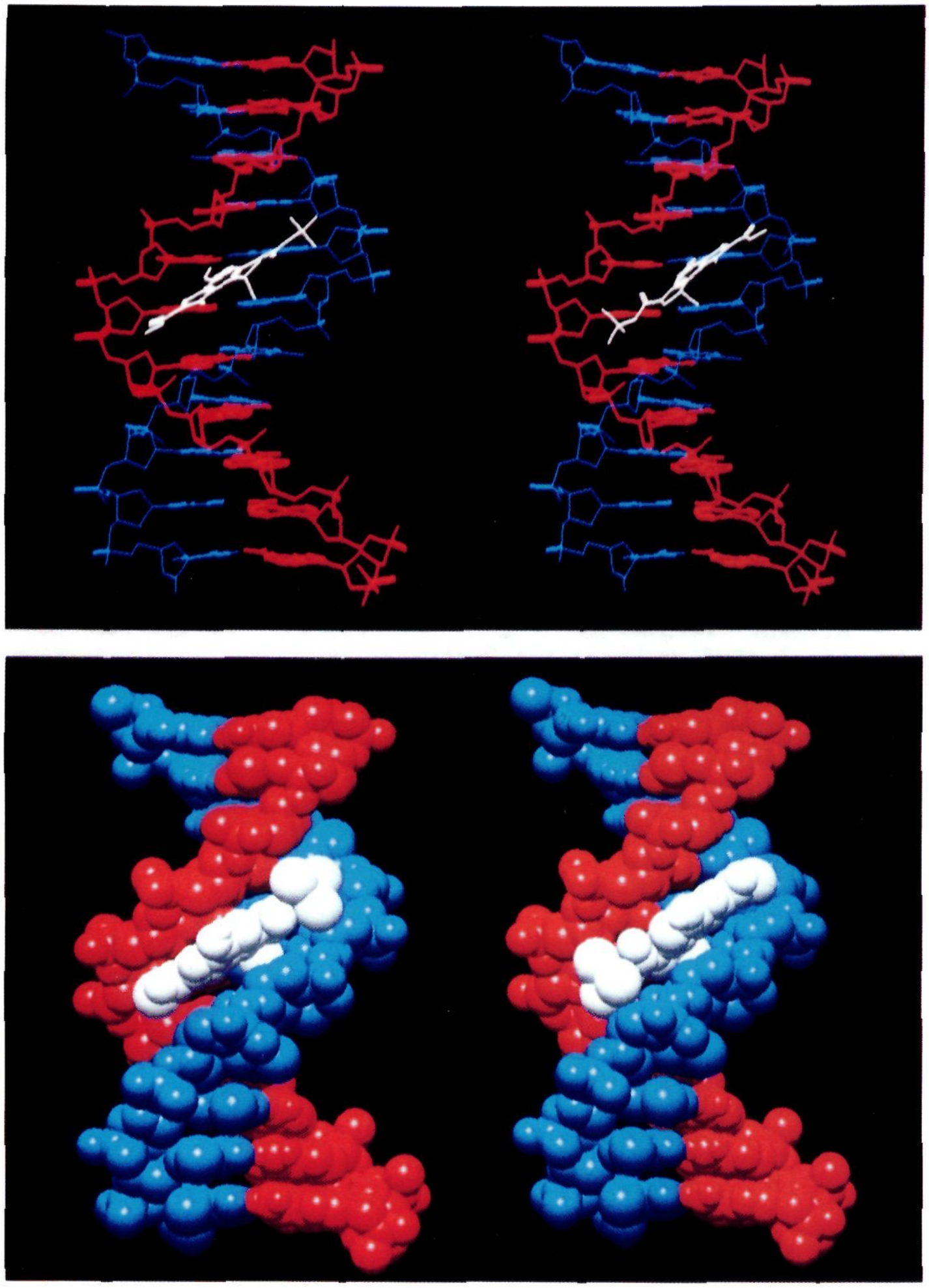

Figure 8. Comparison stick and space-filling models of the (+)-*N*-BOC-DSA (left) and *ent*-(–)-*N*-BOC-DSA (right) alkylation at the same site within w794 DNA (*cf.* Figure 7): duplex 5′-d(GACTAATTTTT). The natural enantiomer binding extends in the 3′→5′ direction from the adenine N3 alkylation site across the site 5′-AA. The unnatural enantiomer binding extends in the 5′→3′ direction but binds across the same 5′-AA site. The model complexes were generated with MacroModel (AMBER force field supplemented with agent parameters).

5′→3′ binding orientation required for adenine N3 access to the activated cyclopropane, Figures 8 and 9. As a consequence of the diastereomeric relationship of the two alkylations, the binding of (–)-**2**, while oriented in the 5′→3′ direction, covers the same adjacent 5′ base as (+)-**2**. Thus, for simple derivatives of either enantiomer of the alkylation subunit, a single adjacent 5′ A or T base is sufficient for observation of DNA alkylation. This has suggested to us that the simple event governing DNA alkylation is the depth of minor groove penetration by the agent and steric accessibility to the adenine N3 alkylation site. For simple derivatives of the alkylation subunits including *N*-BOC-DSA, this requires a single 5′ A or T base adjacent to the adenine alkylation site in order to permit sufficient access for alkylation.

Illustrated in Figure 9 are enlarged models of the central four base-pairs of the natural and unnatural *N*-BOC-DSA enantiomer alkylations of the common 5′-d(GACTAATTTTT) site taken from Figure 8 and their comparisons with an unobserved and hypothetical alkylation at a similar site, 5′-d(GACTGATTTTT), bearing a 5′ G base adjacent to the adenine N3 alkylation site. The C2 amine of the 5′ G which extends into the minor groove sterically precludes either a natural or an unnatural enantiomer alkylation at such a 5′-d(GA) site. Only when the adjacent 5′

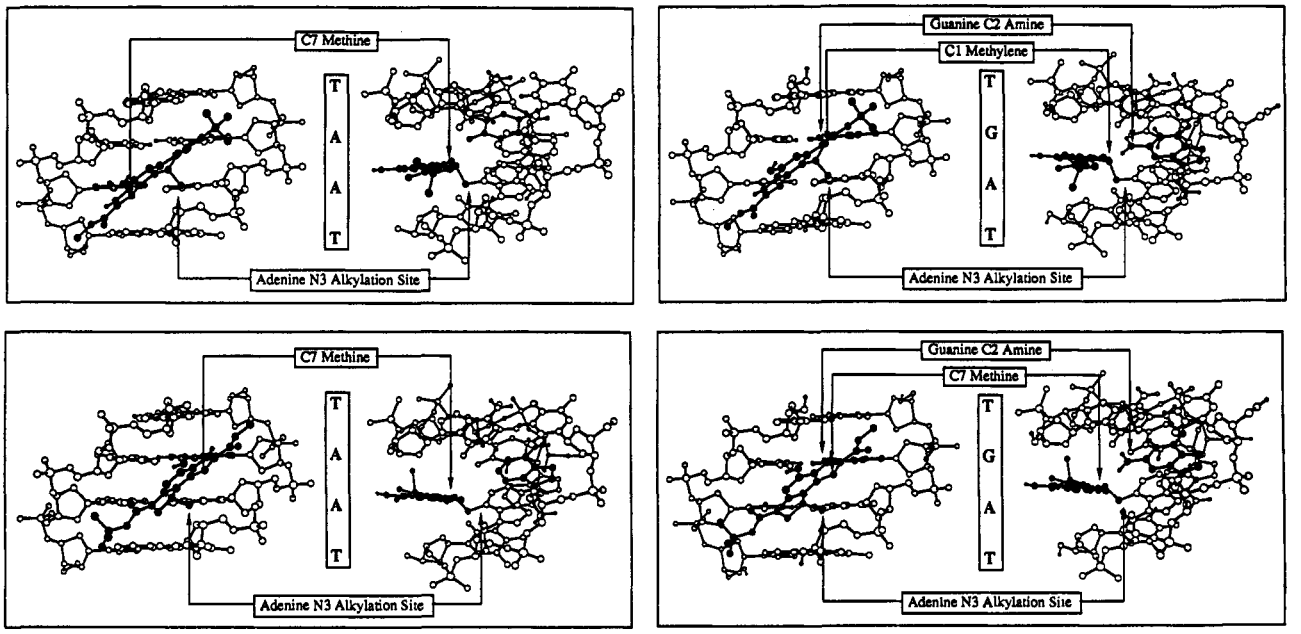

Figure 9. (Top) Expanded and rotated views of the (+)-*N*-BOC-DSA (natural enantiomer) alkylation of the 5′-AA site taken from Figure 8 [5′-d(GACTAATTTTT) alkylation] (left) and a comparable model of a hypothetical 5′-GA alkylation illustrating the destabilizing guanine C2 amine steric interactions that preclude reaction at such a site, C1-CH_2/adjacent 5′ guanine C2-NH_2 distance = 1.55 Å (right). The natural enantiomer binds in the 3′→5′ direction from the adenine N3 alkylation site extending across the 5′-AA site. The C7-H is proximal to the complementary strand thymine (in black) and produces a significant but not serious destabilizing steric interaction, C7-H/thymine C=O distance = 2.26 Å. (Bottom) Expanded and rotated views of the (–)-*N*-BOC-DSA (unnatural enantiomer) alkylation of the 5′-AA site taken from Figure 8 (left) and a comparable model of a hypothetical 5′-GA alkylation illustrating the destabilizing guanine C2 amine steric interactions that preclude reaction at such a site, C7-H/adjacent 5′ G C2-NH_2 distance = 1.51 Å (right). The unnatural enantiomer binds in the reverse 5′→3′ direction but with binding that also covers the same 5′-AA site as the natural enantiomer. The model highlights the unnatural enantiomer sensitivity to the destabilizing steric interactions of the C7 hydrogen substituent with the alkylation site adjacent 5′ adenine (in black) located on the same strand.

base is A or T is sufficient groove penetration possible to permit the adenine N3 alkylation. This fundamentally simple and consistent interpretation is identical to but more refined than that disclosed in our earlier work with enantiomeric CC-1065 agents[28] but differs from that advanced by others,[27] where different polynucleotide recognition features have been counterintuitively suggested to be responsible for the behavior of each of the CC-1065 and CPI enantiomers.

The results have further suggested that the distinctions in the relative efficiency of DNA alkylation by (+)-*N*-BOC-DSA versus (+)-*N*-BOC-CPI may be interpreted simply in terms of steric accessibility to the alkylation site. That is, the C7 methyl group of the CPI[28] subunit sterically destabilizes adduct formation or decelerates the rate of DNA alkylation to the extent that the less reactive but more accessible DSA subunit alkylates DNA more efficiently. As discussed in more detail later on, we also suggest that the unnatural enantiomers are more sensitive to destabilizing C7 substituent steric hindrance of the alkylation reaction as a consequence of its proximal positioning next to the alkylation site adjacent 5′ base (see Figures 8 and 9) and that this single structural feature is responsible for their diminished DNA alkylation properties.

Two additional and fundamentally important observations were made in the examination of the DNA alkylation properties of **2**. Although the reversible *N*-BOC-DSA alkylation reaction proved difficult to assess using the protocol detailed for **1** and **3** due to the concentrations of agent required to detect alkylation, incubation of (+)-**2** with calf thymus DNA (1:80 agent:bp ratio) established the readily reversible nature of the adduct formation. Following incubation of (+)-**2** with calf thymus DNA (25 °C, 3 days), the unreacted agent was removed by exhaustive EtOAc extraction, and the preparative isolation of the alkylated DNA was accomplished by EtOH precipitation. Redissolution of the alkylated DNA in buffer (10 mM Na_2HPO_4–NaH_2PO_4, pH 7.0, 25 °C), EtOAc extraction of the incubation mixture at 1-day, 3-day, 6-day, and 12-day intervals and HPLC identification and quantitation of the released (+)-*N*-BOC-DSA revealed that the reversal of the DNA alkylation reaction which followed simple first-order kinetics was 50% complete in 24 h at pH 7.0. Thus, (+)-duocarmycin SA required conditions of 50 °C, pH 8.4, 24 h for observation of 50% reversal of an established alkylation (Figure 4) while 25 °C, pH 7.0, 24 h was sufficient for 50% reversal of the (+)-*N*-BOC-DSA alkylation of calf thymus DNA. Consistent with expectations, this faster rate of retroalkylation and lower degree of adduct stability observed with (+)-**2** versus (+)-**1** may be attributed to the lack of the noncovalent binding stabilization in (+)-**2** provided by the trimethoxyindole subunit of (+)-**1**.

In addition, incubation of (+)-**2** with the calf thymus DNA (1:80 agent:bp ratio) at 25 °C (24 h) versus 37 °C (72 h) led to the observation that thermal depurination occurs to a surprisingly substantial extent at 37 °C. Under the incubation conditions of 25 °C (24 h) approximately 80% of the (+)-*N*-BOC-DSA was recovered unchanged from the incubation mixture by EtOAc extraction. Thermolysis (100 °C, 30 min) of the alkylated DNA led to isolation of approximately 20% adenine adduct resulting from depurination. In contrast, little (+)-**2** (<5%) was recovered from the 37 °C, 72 h incubation mixture by EtOAc extraction and the (+)-*N*-BOC-DSA–adenine adduct was isolated directly (55%). Subsequent thermolysis of the alkylated DNA (100 °C, 30 min) led to isolation of only 45% additional adenine adduct resulting from depurination. Of the total amount of adenine adduct isolated resulting from depurination, 55% was obtained directly from EtOAc extraction of the initial 37 °C incubation mixture, and only an additional 45% was obtained following the deliberate thermal depurination conducted at 100 °C. Consequently, over half of the detected depurination reaction occurred at 37 °C under the initial incubation conditions. To us, this has suggested that the detection of the readily reversible *N*-BOC-DSA DNA alkylation reaction with use of end-labeled DNA (sequencing studies) results in a large measure from adventitious depurination under the initial incubation conditions (37 °C, 24 h). Although the intensity or efficiency of such alkylations conducted at 37 °C may represent an accurate measure of the

relative extent, rate or stability of the DNA alkylation among structurally related agents (*i.e.*, *N*-BOC-DSA, -CPI, -CBI), they cannot be taken to be a quantitative measure of the extent of DNA alkylation at the time of the deliberate thermal depurination and strand cleavage reaction (100 °C). In addition, the relative biological importance of the initial alkylative modification of DNA versus depurination under physiological conditions (37 °C) also remains to be established.

***ent*-(−)-Duocarmycin SA.** Through the efforts of chemical synthesis which provided our samples of (+)-duocarmycin SA and the BOC derivatives of the DSA alkylation subunit, *ent*-(−)-duocarmycin SA was available for examination.[21] In our preliminary studies, *ent*-(−)-duocarmycin SA was found to be a potent cytotoxic agent (100 pM, L1210) that proved to be only 10 times less potent than the natural enantiomer. Consistent with this observation, *ent*-(−)-duocarmycin SA and its corresponding seco derivative were found to alkylate duplex DNA at concentrations approximately 10 times that of the natural enantiomer, and it was found to occur with a readily distinguishable alkylation profile, Figure 7. Table 2 summarizes the composite consensus sequence of the alkylation sites observed for *ent*-(−)-duocarmycin SA, and Figure 2 illustrates the comparison alkylation profiles of (+)- and (−)-**1** within the segments of DNA examined. Notably, each of the alkylation sites proved to be adenine, and no minor guanine alkylation was detected. Both the rate and the intensity of the *ent*-(−)-duocarmycin SA alkylation were lower than those of the natural enantiomer, and the detection of the unnatural enantiomer alkylation required more vigorous and prolonged incubation conditions (25 °C, 1–6 days). In sharp contrast to (+)-**1**, where little distinction in the relative intensity of DNA alkylation was detected between 4 and 25 °C reactions (24 h), only slow alkylation was observed with (−)-**1** in reactions conducted at 4 °C (1–4 days). Representative of this distinction, the relative rates of alkylation at the single high affinity alkylation sites within w794 DNA (Figure 7) for (+)- and *ent*-(−)-duocarmycin SA were measured with reactions conducted under identical conditions (10^{-5} M agent, 25 °C). (+)-Duocarmycin SA was determined to alkylate the 5′-AATTA site at a rate approximately 50 times greater than the (−)-duocarmycin SA alkylation of the 5′-AATTT site, $k(+)/k(-) = 48$ (Figure 11, Experimental Section). As a consequence of this significantly diminished rate and efficiency of DNA alkylation, the assay of *ent*-(−)-duocarmycin SA conducted over a 10 000-fold concentration range always exhibited minor cleavage sites attributable to the natural enantiomer despite the exceptional enantiomeric purity of the sample (≥99.9%).[21] This unavoidable contamination by the natural enantiomer alkylation complicates the interpretation of the (−)-**1** alkylation selectivity. Thus, while the unique and/or high affinity alkylation sites for *ent*-(−)-duocarmycin SA were readily established in our studies, the minor alkylation sites observed should be interpreted with more caution. It is likely that the extended weak A–T preference on the 5′ side of the adenine alkylation site illustrated in Table 2 is overestimated and reflects the unavoidable inclusion of contaminating natural enantiomer sites. Similarly, the AT-rich selectivity observed to the 3′ side of the adenine alkylation site may be underestimated due to this same feature.[45] Nonetheless, the high affinity alkylation sites and especially the unique sites for *ent*-(−)-duocarmycin SA proved readily detectable, and each proved consistent with 5′ adenine alkylation, agent binding in the minor groove in the 5′→3′ direction from the alkylation site covering 3.5 base-pairs across an AT-rich region. *All* alkylation sites detected proved to be adenine and nearly all of the 3′ and 5′ bases flanking the adenine N3 alkylation site proved to be A or T, Tables 2 and 6. The six exceptions to this generalization represent a tolerance for a 3′ cytosine adjacent to a 5′-TA alkylation site or a 5′ cytosine adjacent to a 5′-AA alkylation site. Like the natural enantiomer, there proved to be a preference for this three-base sequence which follows the order 5′-AAA > 5′-AAT > 5′-TAA > 5′-TAT (Table 6), with a pronounced preference for the sequence 5′-AAA. There also proved to be a weak preference for the second 3′ base to be A or T versus G or C. At least part of origin for the preference for the enriched A versus mixed AT-rich sites for *ent*-(−)-duocarmycin SA (5′-AAA > 5′-AAT, 5′-TAA > 5′-TAT), also observed with *N*-BOC-DSA (5′-AA > 5′-TA) and (+)-duocarmycin SA (5′-AAA > 5′-TTA > 5′-TAA > 5′-ATA), lies in the statistically relevant opportunity for alkylation of a complementary strand adenine within the mixed AT-rich sequences competitive with the labeled strand site. Presumably, this competitive complementary strand alkylation would preclude an additional labeled strand alkylation within the same overlapping site and lower the apparent alkylation efficiency.

Although this (−)-duocarmycin SA AT-rich alkylation selectivity relative to the adenine N3 alkylation site is offset from that observed with (+)-duocarmycin SA, it is the natural consequence of the diastereomeric relationship of the adducts and is fully consistent with a binding orientation that extends in the 5′→3′ direction. Thus, the *ent*-(−)-duocarmycin SA DNA alkylation proved to be analogous to that of (+)-duocarmcyin SA with the exception that the unnatural enantiomer binding direction (5′→3′) across an AT-rich region is reversed and offset from that observed with the natural enantiomer (3′→5′).

Quantitation, Isolation, and Characterization of the (−)-Duocarmycin SA–Adenine Adduct. The confirmation of the structural nature of the (−)-duocarmycin SA adenine N3 alkylation was accomplished through isolation, quantitation, and characterization of the unnatural enantiomer of the thermally released adduct **4**. Thus (−)-**1** was reacted with calf thymus DNA in the same manner described for (+)-**1** except that the incubation period (25 °C) was extended to 3 days. The (−)-duocarmycin SA–adenine adduct **4** was isolated as the only detectable UV active product from the thermal depurination reaction, purified by chromatography (SiO_2, 0–10% CH_3OH–CH_2Cl_2 gradient elution, 92%), and it proved to be identical in all respects to (+)-**4** (^1H NMR, TLC, HPLC, UV, HRMS) but was found to possess the opposite stereochemistry (CD, $[\alpha]_D$). The ^1H NMR of (−)-**4** is illustrated in Figure 3. Notably, (−)-**4** was isolated by EtOAc extraction both prior to the thermal depurination reaction (6%) and after thermal treatment (100 °C, 30 min, an additional 86%). Therefore, depurination occurred to a small extent under the incubation conditions (25 °C, 3 days) even before the thermal depurination reaction (100 °C, 30 min). Thus, through isolation, quantitation, and characterization of (−)-**4**, the adenine N3 alkylation by (−)-duocarmycin SA was found to account for 92% of the consumption of the agent in the presence of duplex DNA and constitutes the predominant if not exclusive alkylation event under the conditions examined (agent: base-pair ratio of 1:100).

There are two additional and important ramifications of the observation of the slow depurination at 25 °C resulting from the adenine N3 alkylation. The first and most obvious is that the reaction of (+)- or (−)-duocarmycin SA and related agents including CC-1065 and its analogs results not only in alkylative modification of duplex DNA but also in slow depurination and potential strand cleavage under physiological conditions (37 °C). The relative biological importance of the simple alkylative modification of DNA versus the resulting depurination and strand cleavage remains to be established. In addition, it is an especially important observation in regard to the detectability of the *N*-BOC-DSA DNA alkylation reaction. Not only is the *N*-BOC-DSA DNA alkylation detectable only at concentrations 10^4–10^5 times greater than that of (+)-duocarmycin SA, but the detection of

(45) Interestingly, (+)-CC-1065, (+)-duocarmycin SA and A exhibit a detectable but weaker A-T preference to the 3′ side of the alkylation site and an occasional G or C base within the two 5′ bases adjacent to the alkylation site. It is tempting to suggest that these observations similarly reflect the detection of contaminant unnatural enantiomer alkylations over the 10 000-fold concentration range studied despite the enantiomeric purity of the agents (≥99.9%). However, since the natural enantiomer alkylations have proven kinetically faster and more efficient, the potential unnatural enantiomer contamination of the perceived alkylation selectivity is minimal.

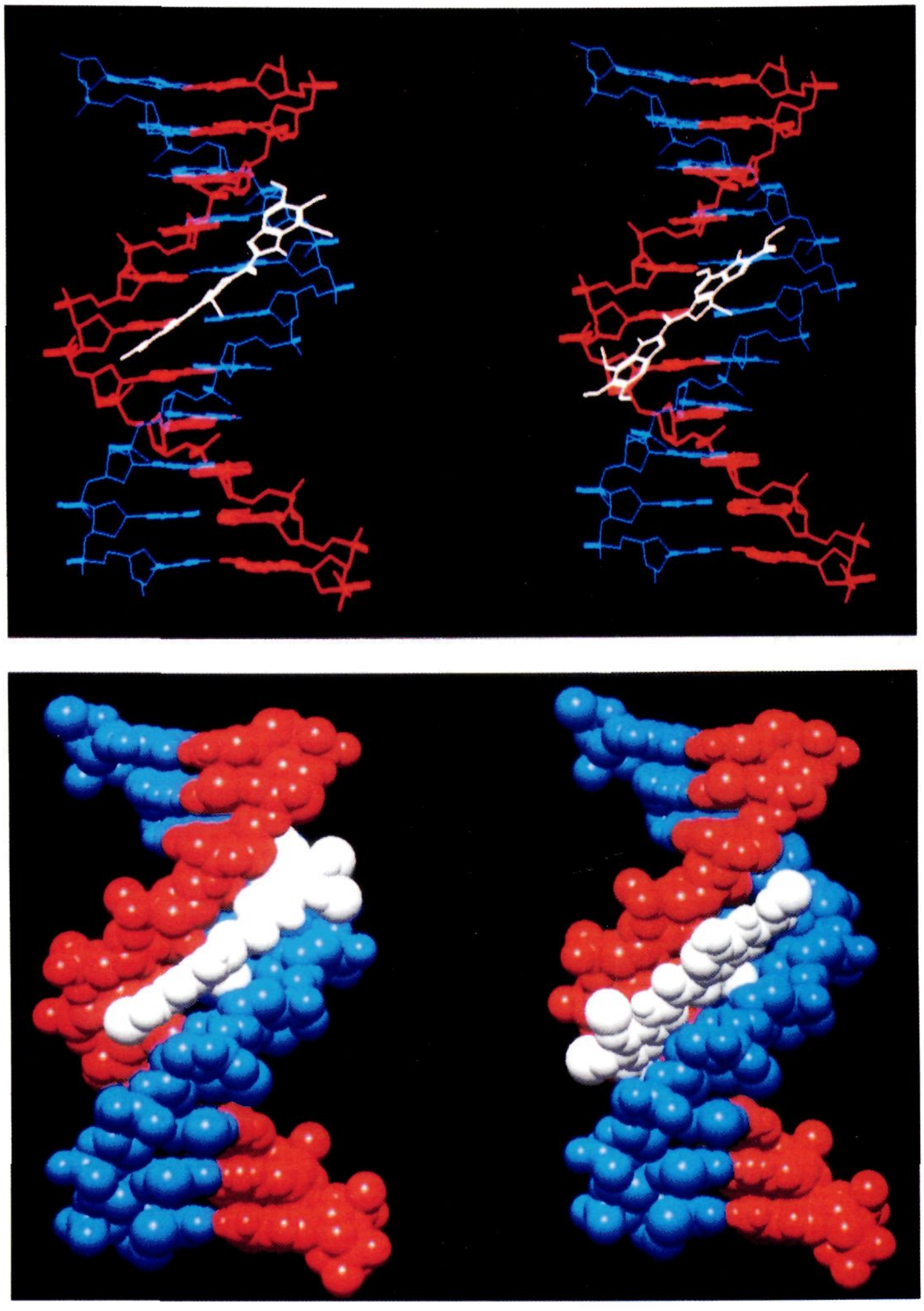

Figure 10. Comparison stick and space-filling models of the (+)-duocarmycin SA (left) and *ent*-(–)-duocarmycin SA (right) alkylation at the same site within w794 DNA: duplex 5′-d(GACTAATTTTT). The natural enantiomer binding extends in the 3′→5′ direction from the adenine N3 alkylation site across the site 5′-CTAA. The unnatural enantiomer binding extends in the 5′→3′ direction across the site 5′-AATT. The model complexes were generated with MacroModel (AMBER force field supplemented with agent parameters) and subjected to full complex minimization.

the alkylation reaction also requires the use of more vigorous reaction conditions and extended reaction times (37 °C, 24–48 h). It is likely that *N*-BOC-DSA rapidly and readily reversibly alkylates duplex DNA but that the use of vigorous reaction conditions (37 °C) results in detectable depurination under the incubation conditions of the assay.

Concurrent with these efforts, we also conducted a series of studies to determine whether the unnatural enantiomer diminished intensity of DNA alkylation was simply the result of a lower rate or efficiency of DNA alkylation or was due to enhanced reversibility which lowers the extent of DNA alkylation detected. In these studies, we found that the use of TE buffer (pH 7.5 > 8.2, 5.9; 100 °C, 30 min) proved especially effective and provided stoichiometric depurination with no detected reversible reaction. The use of 10 mM phosphate buffer at pH 7.0 (100 °C, 30 min) proved to be nearly as effective, but TE buffer with 0.25 M NaCl (pH 7.9) or 250 mM phosphate buffer (pH 7.5) proved to be significantly less effective. Thus, for the sequencing studies, thermal cleavage conducted in TE buffer (pH 7.0–7.5) has proven especially effective, while the use of 10 mM phosphate buffer (pH 7.0) has proven equally effective and especially useful for preparative reactions designed to permit isolation of the depurination product free of extraction impurities derived from buffer.

Table 6. Summary of DNA Alkylation Sites for (–)-Duocarmycin SA

sequence	no. total sites	no. alkylation sites
5′-(NAAN)-3′	82	40 (49%)
5′-(NAAA)-3′	39	33 (85%)
5′-(NAAT)-3′	15	7 (47%)
5′-(NAAG)-3′	15	0 (0%)
5′-(NAAC)-3′	13	0 (0%)
5′-(NTAN)-3′	54	13 (24%)
5′-(NTAA)-3′	18	7 (39%)
5′-(NTAT)-3′	15	4 (27%)
5′-(NTAG)-3′	12	0 (0%)
5′-(NTAC)-3′	9	2 (22%)
5′-(NGAN)-3′	30	0 (0%)
5′-(NGAA)-3′	11	0 (0%)
5′-(NGAT)-3′	4	0 (0%)
5′-(NGAG)-3′	12	0 (0%)
5′-(NGAC)-3′	3	0 (0%)
5′-(NCAN)-3′	50	4 (8%)
5′-(NCAA)-3′	13	4 (31%)
5′-(NCAT)-3′	13	0 (0%)
5′-(NCAG)-3′	17	0 (0%)
5′-(NCAC)-3′	7	0 (0%)

sequence	no. AS/no. TS[a]	high affinity[b]	low affinity[b]
5′-(NAAAN)-3′	33/39 (85%)	25 (64%)	8
5′-(NAATN)-3′	7/15 (47%)	3 (20%)	4
5′-(NTAAN)-3′	7/18 (39%)	1 (6%)	6
5′-(NTATN)-3′	4/15 (27%)	0 (0%)	4
5′-(NAAAN)-3′			
5′-(NAAAA)-3′	19/21 (90%)	15 (71%)	4
5′-(NAAAT)-3′	5/7 (71%)	3 (43%)	2
5′-(NAAAG)-3′	8/9 (89%)	6 (67%)	2
5′-(NAAAC)-3′	1/2 (50%)	1 (50%)	0
5′-(NAATN)-3′			
5′-(NAATA)-3′	2/5 (40%)	1 (20%)	1
5′-(NAATT)-3′	4/5 (80%)	2 (40%)	2
5′-(NAATG)-3′	1/2 (50%)	0 (0%)	1
5′-(NAATC)-3′	0/3 (0%)	0 (0%)	0
5′-(NTAAN)-3′			
5′-(NTAAA)-3′	3/6 (50%)	1 (17%)	2
5′-(NTAAT)-3′	0/3 (0%)	0 (0%)	0
5′-(NTAAG)-3′	0/3 (0%)	0 (0%)	0
5′-(NTAAC)-3′	4/6 (67%)	0 (0%)	4
5′-(NTATN)-3′			
5′-(NTATA)-3′	1/6 (17%)	0 (0%)	1
5′-(NTATT)-3′	2/4 (50%)	0 (0%)	2
5′-(NTATG)-3′	1/5 (20%)	0 (0%)	1
5′-(NTATC)-3′	0/0		

[a] Number of alkylated sites/number of total sites. [b] Intensity of alkylation at the sites: high = high affinity site observed at lowest agent concentration; low = low affinity site observed at higher agent concentrations. The expressed percentage is that of the number of high affinity alkylation sites per number of total sites.

Model of the (–)-Duocarmycin SA DNA Alkylation. Given the structural confirmation of the adenine N3 adduct in which the least substituted cyclopropane carbon was found to be alkylated, the established absolute configuration of the agent,[21] and the AT-rich selectivity of the alkylation which extends in the 5′→3′ direction from the adenine alkylation site, a model of the (–)-duocarmycin SA alkylation of duplex DNA may be constructed. This is illustrated in Figure 10 with the w794 site 5′-(GACTAATTTTT), which constitutes the high affinity site for (–)-duocarmycin SA and a minor alkylation site for (+)-duocarmycin SA.

For both enantiomers, the hydrophobic concave face of the agent is bound deeply in the minor groove across an AT-rich region, the polar functionality of the agent lies on the outer face of the complex, and the agents adopt a bound helical conformation that follows the curvature and pitch of the minor groove covering 3.5 base-pairs. The difference in the two models is that (–)-duocarmycin SA binds in the reverse 5′→3′ direction from the site of alkylation while (+)-duocarmycin SA binds in the 3′→5′ direction from the same site. In this regard, the natural enantiomer model illustrated in Figure 10 is analogous to that shown in Figure 6. For (+)-duocarmycin SA, the binding spans 3.5 base-pairs starting with the 3′ adenine alkylation site and extends in the 3′→5′ direction over the 2–3 adjacent 5′ base pairs (5′-CTAA). For (–)-duocarmycin SA, the binding similarly spans a 3.5 base-pair AT-rich site, but which necessarily starts at the 5′ base adjacent to the alkylation site and extends in the 5′→3′ direction to cover the adenine alkylation site and the 1–2 adjacent 3′ base-pairs (5′-AATT). Notable is the fact that this offset alkylation selectivity within an AT-rich site is the natural consequence of the diastereomeric relationship of the alkylated DNA, the required reversed binding orientation of the agents in the minor groove to permit adenine N3 access to the electrophilic cyclopropane, and the model embodies the inherent deep groove penetration of the full bound agent at the appropriate AT-rich 3.5 base-pair site surrounding the alkylation site. In addition, the (–)-duocarmycin SA binding illustrated in Figure 10 spans a four base AT-rich site 5′-(AATT), while the (+)-duocarmycin SA binding spans a three base AT-rich site 5′-(CTAA). The relative importance or preference of the fourth base (A/T > G/C) in the binding sequences is presumably the reason this site constitutes a high affinity site for the unnatural enantiomer but only a minor site for the natural enantiomer.

Origin of the Distinctions in the Natural and Unnatural Enantiomer DNA Alkylation Capabilities. The studies have suggested an attractive explanation for the sometimes confusing behavior (relative DNA alkylation efficiency, relative biological potency) of pairs of enantiomeric agents which we believe may be traced to a single structural feature—the relative degree of steric bulk surrounding the duocarmycin SA C7 center within the alkylation subunit for which the unnatural enantiomers are especially sensitive. The enantiomer distinctions have proven readily detectable with the simple alkylation subunits themselves (*i.e.*, *N*-BOC-DSA, –CI, –CPI, –CBI), are most prominent with the dimer-based agents (*i.e.*, duocarmycin SA, duocarmycin A, CBI-CDPI$_1$, CPI-CDPI$_1$, CPI-PDE-I$_1$, Table 7), and are less prominent with the larger trimer- or tetramer-based agents (*i.e.*, CC-1065, CPI-CDPI$_2$, CBI-CDPI$_2$, CPI-CDPI$_3$).[28] In general, less distinction in the biological potency and relative DNA alkylation efficiency has been observed with the CI and duocarmycin SA enantiomeric pairs, both of which lack substituents or steric bulk at this position within the alkylation subunit. Moreover, the distinctions among enantiomeric CI-based agents which lack the pyrrole ring altogether are generally smaller than those observed with the duocarmycin SA-derived agents (DSA > CI). In contrast, the CPI-, CBI-, and duocarmycin A-based agents generally exhibit more pronounced distinctions within enantiomeric pairs (CPI > CBI > duocarmycin A), and each possesses a substituent or inherent steric bulk at this position (CPI > CBI > duocarmycin A). We believe that the distinguishing behavior of the unnatural enantiomer of duocarmycin SA as well as that of all agents studied to date is derived from a pronounced steric interaction of the C7 center with the 5′ base adjacent to the adenine N3 alkylation site necessarily present with the 5′→3′ binding of the unnatural enantiomers, see Figures 8–10. The 3′→5′ binding model for the natural enantiomers benefits from a less substantial but still potentially significant sensitivity to steric bulk at this same C7 position.

Consistent with the empirical observations to date and in agreement with models of the alkylation adducts, the studies suggest that agents lacking steric bulk surrounding the position occupied by a duocarmycin SA C7 substituent are predictably more effective at alkylating DNA (rate and/or intensity), that the unnatural enantiomers of such agents are especially sensitive to steric bulk at this position, and that as this steric bulk is reduced, the distinguishing features of the enantiomers (efficiency of DNA alkylation, biological potency) diminish.

Trace Guanine Alkylation. Recent studies have detailed the detection of a trace or minor guanine N3 alkylation with (+)-

Table 7. Natural and Unnatural Enantiomer Distinctions

agent	configuration	IC_{50} (ng/mL) L1210	rel. IC_{50}	DNA (+)/(-)[a]
(+)-CI-CDPI$_1$	natural	10	1	0.5–2.0
(-)-CI-CDPI$_1$	unnatural	20	0.5	
(+)-duocarmycin SA	natural	0.006	1	10
(-)-duocarmycin SA	unnatural	0.06	0.1	
(+)-duocarmycin A	natural	0.1	1	>100
(-)-duocarmycin A	unnatural	>10	<0.01	
(+)-CBI-CDPI$_1$	natural	0.002	1	>100
(-)-CBI-CDPI$_1$	unnatural	>2	<0.001	
(+)-CPI-CDPI$_1$	natural	0.02	1	>100
(-)-CPI-CDPI$_1$	unnatural	>3	<0.006	

[a] Relative efficiency of the natural(+)/unnatural(-) enantiomer DNA alkylation within w794 DNA (25 °C, 24 h).

duocarmycin A.[17,18] From the reports to date, the relative importance or extent of this minor guanine reaction has not always been evident. Under conditions of limiting agent (1:70 agent:base-pair ratio), the preparative isolation of the thermally released (+)-duocarmycin A-adenine adduct was shown to account for 86–92% of the consumption of the agent.[8] Similarly, two groups have independently established that all alkylation and subsequent thermal cleavage events detected to date within end-labeled restriction fragments on sequencing gels occurs at adenine.[8,18] In this latter protocol, high affinity and minor alkylation sites are detected, while trace alkylation events are not detectable due to competing multiple alkylations of the duplex DNA which lead to its complete consumption and the production of only short segments of DNA. To date, the minor (+)-duocarmycin A guanine N3 alkylation has been detected only upon isolation of the thermally released adduct following treatment of DNA with excess agent,[17] within oligonucleotides lacking a high affinity duocarmycin A alkylation site,[17] or when the adenine alkylation sites within AT-rich regions of duplex DNA are prebound and protected from alkylation with high affinity AT-rich minor groove binding agents including distamycin.[18] Consequently, it was of interest to determine what effect the enhanced stability and selectivity of (+)-duocarmycin SA would have on the detectability of this trace, minor guanine N3 alkylation observed with (+)-duocarmycin A.

Incubation of (+)-duocarmycin SA with calf thymus DNA (1:7 agent:base-pair ratio) was carried out under the same conditions (37 °C, 9 and 24 h) for which (+)-duocarmycin A has been reported to provide a 1:1 mixture of adenine (41%) and guanine (39%) adducts.[17] EtOAc extraction of the mixture to remove unreacted (+)-**1** (28% after 9 h; 20% after 24 h), thermolysis of the covalently modified DNA (100 °C, 60 min), and EtOAc extraction of the mixture to isolate the duocarmycin SA–adenine adduct **4** and the corresponding guanine N3 adduct provided **4** (60% after 9 h, 68% after 24 h) as the near exclusive UV active product. Only two additional products were detectable in trace amounts (1 and 3%) by reverse-phase HPLC (VYDAC C_{18}, 5 μm, 0.46 × 25 cm, 10–50% CH_3CN–0.05 M HCO_2NH_4 linear gradient). Given the trace quantities of the minor products, no effort could be made to isolate and characterize the materials. However, the study did illustrate that a competing guanine alkylation cannot account for more than a trace amount of the consumption of the agent (adenine:guanine N3 alkylation > 25:1) even under demanding alkylation conditions (37 °C) employing excess agent. Notably, (+)-**1** (20–28%) was recovered from the incubation mixture, and the adenine N3 alkylation accounted for 84–90% of the consumption of agent even under these vigorous conditions. Thus, (+)-duocarmycin SA exhibits a substantially more selective reactivity for adenine versus guanine alkylation to the extent that in the absence of a productive adenine alkylation site no significant competitive reaction is observed.[46] This enhanced alkylation selectivity of **1** may be attributed to its diminished reactivity. Since (+)-duocarmycin SA is substantially more potent than (+)-duocarmycin A, the competing guanine N3 alkylation cannot by uniquely relevant to the expression of the biological properties of this class of agents and may, in fact, represent a nonproductive competitive event.

Conclusions. The (+)-duocarmycin SA DNA alkylation selectivity was found to be identical to that detailed for (+)-duocarmycin A[8] with the exception that (+)-duocarmycin SA displays an enhanced selectivity among the available alkylation sites and a greater alkylation efficiency (intensity), both attributable to its diminished chemical reactivity (enhanced stability). Each alkylation site detected proved to be adenine flanked by two 5′ A or T bases with a preference that follows the order of 5′-AA<u>A</u> > 5′-TT<u>A</u> > 5′-TA<u>A</u> > 5′-AT<u>A</u> and with the additional preferences for a fourth 5′ base to be A/T versus G/C and a 3′ Pu versus Py base preceding the alkylation site.

The quantitation, isolation, and full characterization of the (+)-duocarmycin SA–adenine adduct thermally released from duplex DNA was shown to account for 90–100% of the consumption of the agent in the presence of duplex DNA under the conditions of limiting agent (agent:base-pair ratio of 1:70) and served to unambiguously establish the alkylation reaction as adenine N3 addition to the unsubstituted carbon of the activated cyclopropane.

The reversibility of the (+)-duocarmycin SA DNA alkylation reaction was defined and compared to those of (+)-duocarmycin A and (+)-CC-1065. The ease or rate of reversibility was found to increase with increasing temperature, pH, and salt concentration, and the relative rate of reversibility proved to decrease and correlate with the relative reactivity of the agent (stability of adduct) as well as the extent of the noncovalent binding stabilization. A fundamental role that this degree of reversibility may play in the expression of the biological properties is proposed, and it is suggested that the simple event of noncovalent binding stabilization of the near thermal neutral and readily reversible adenine N3 alkylation potentiates the cytotoxic activity of the agents.

The first disclosure and comparison of the DNA alkylation properties of both enantiomers of the duocarmycin SA alkylation subunit, *N*-BOC-DSA, were reported. In addition to demonstrating that their DNA alkylation reaction is substantially less efficient (*ca.* 10^4–10^5 times lower), is less selective (5′-A<u>A</u>Pu > 5′-T<u>A</u>Pu), and proceeds with an altered profile in comparison to either (+)- or (-)-duocarmycin SA, the studies demonstrated that the two enantiomers alkylate the same sites within duplex DNA with the same relative efficiency (intensity). These unusual observations are the natural consequence of the alkylation sites being inherent in the DNA rather than the agent structure and the resulting diastereomeric relationship of the adducts. The natural enantiomer binds in the minor groove in the 3′→5′ direction from the site of alkylation extending over the adjacent 5′ base, while the unnatural enantiomer binds with the reverse orientation (5′→3′) but with binding that also necessarily covers

(46) In addition, treatment of poly(dG)–poly(dC) with (+)-duocarmycin SA (1:10 agent:base-pair ratio) under similar conditions (25 °C, 24 h, 10 mM Na_2HPO_4–NaH_2PO_4, pH 7) provided mainly recovered **1** and only trace amounts of additional products.

the same adjacent 5′ base. The observations suggest that the simple event governing alkylation is the steric accessibility to the adenine N3 alkylation site, which in turn is dependent upon the depth of the minor groove penetration by the agent at the alkylation site. For simple derivatives of either enantiomer of the duocarmycin SA alkylation subunit, this requires a single 5′ A or T base adjacent to the adenine N3 alkylation site.

The readily reversible nature of the (+)-*N*-BOC-DSA DNA alkylation reaction was established, and the lower degree of adduct stability observed with (+)-**2** versus (+)-**1** may be attributed to the lack of the noncovalent binding stabilization in (+)-**2** provided by the trimethoxyindole subunit of (+)-**1**. In addition, substantial thermal depurination resulting from DNA alkylation was observed at 37 °C with (+)-*N*-BOC-DSA and duocarmycin SA. The relative biological importance of alkylative modification of duplex DNA versus subsequent depurination under physiological conditions (37 °C) remains to be established.

The first disclosure and subsequent comparative study of the DNA alkylation properties of an unnatural duocarmycin enantiomer, *ent*-(−)-duocarmycin SA, were described. *ent*-(−)-Duocarmycin SA was shown to alkylate DNA at a substantially slower rate (*ca.* 50 times slower) and with a relative efficiency (intensity) that is 10 times lower than that of the natural enantiomer, corresponding nicely with the fact that it is 10 times less potent in cytotoxic assays. When the DNA alkylation reaction was taken to completion, the (−)-duocarmycin SA–adenine adduct thermally released from DNA was shown to account for 92% of the consumption of agent in the presence of duplex DNA under the conditions of limiting agent (agent:base-pair ratio of 1:100). The isolation and characterization of the adduct **4** served to establish the alkylation reaction as proceeding by adenine N3 addition to the least substituted carbon of the activated cyclopropane.

The unnatural enantiomer alkylation was also determined to proceed with a readily distinguishable profile. Each alkylation site proved to be adenine, and nearly all of the 5′ and 3′ bases flanking the adenine N3 alkylation site proved to be A or T. There proved to be a preference for this three-base AT-rich sequence that follows the order 5′-A<u>A</u>A > 5′-A<u>A</u>T > 5′-T<u>A</u>A > 5′-T<u>A</u>T. There also proved to be a weak preference for the second 3′ base to be A or T versus G or C. In this regard, the *ent*-(−)-duocarmycin SA alkylation proved to be analogous to the natural enantiomer alkylation with the exception that the binding orientation is reversed (5′→3′) over an AT-rich 3.5 base-pair site. However, while the bound conformation of the natural enantiomer covers an AT-rich 3.5 base-pair site extending from the adenine N3 alkylation site in the 3′→5′ direction across the adjacent two to three 5′ bases (*i.e.*, 5′-AAA<u>A</u>), the AT-rich 3.5 base-pair site for the unnatural enantiomer extends in the reverse 5′→3′ direction, necessarily starting at the first 5′ base site preceding the adenine N3 alkylation site and extending across the alkylation site to the first and second adjacent 3′ bases (*i.e.*, 5′-A<u>A</u>AA). The reversed binding orientation is required to permit adenine N3 access to the electrophilic cyclopropane, and the offset AT-rich alkylation selectivity is the natural consequence of the diastereomeric relationship of the adducts.

Comparative three-dimensional models of the natural and unnatural enantiomer alkylations were presented and clearly illustrate the offset binding sites required to accommodate the enantiomer alkylations. Thus, a fundamentally simple and fully consistent model for the duocarmycin DNA alkylation reaction *that accommodates the behavior of both enantiomers* was detailed in which the sequence selectivity of the DNA alkylation reaction is derived from the noncovalent binding selectivity of the agents preferentially within the narrower, sterically more accessible AT-rich minor groove, the inherent steric accessibility to the adenine N3 alkylation site that accompanies deep penetration of the agent into the minor groove within an AT-rich site, and the 3.5 base-pair binding site size required to permit full agent binding in the minor groove at the alkylation site.

Using these models, an explanation for the distinguishing DNA alkylation rate and efficiency as well as the biological potency of enantiomeric pairs of agents was detailed on the basis of the unnatural enantiomer sensitivity to steric bulk at the duocarmycin SA C7 center.

Finally, a study of the (+)-duocarmycin SA DNA alkylation under the conditions of excess agent and limiting DNA revealed that the adenine:guanine N3 alkylation selectivity is >25:1 even under vigorous reaction conditions (37 °C).

Experimental Section

DNA Alkylation Studies of 1–3. Selectivity. General procedures, the preparation of singly 5′ end-labeled double-stranded DNA, the agent binding studies, gel electrophoresis, and autoradiography were conducted according to procedures described in full detail elsewhere.[29] Eppendorf tubes containing the 5′ end-labeled DNA[29] (9 μL) in TE buffer (10 mM Tris, 1 mM EDTA, pH 7.5) were treated with the agent in DMSO (1 μL at the specified concentration). The solution was mixed by vortexing and brief centrifugation and subsequently incubated at 4 or 25 °C (**3** and **1**) or 37 °C (**2**) for 24 h. The covalently modified DNA was separated from unbound agent by EtOH precipitation and resuspended in TE buffer (10 μL). The solution of DNA in an Eppendorf tube sealed with parafilm was warmed at 100 °C for 30 min to induce cleavage at the alkylation sites, allowed to cool to 25 °C, and centrifuged. Formamide dye (0.03% xylene cyanol FF, 0.03% bromophenol blue, 8.7% Na_2EDTA 250 mM) was added (5 μL) to the supernatant. Prior to electrophoresis, the sample was denatured by warming at 100 °C for 5 min, placed in an ice bath, and centrifuged, and the supernatant (3 μL) was loaded directly onto the gel. Sanger dideoxynucleotide sequencing reactions were run as standards adjacent to the reaction samples. Polyacrylamide gel electrophoresis (PAGE) was run on an 8% sequencing gel under denaturing conditions (8 M urea) in TBE buffer (100 mM Tris, 100 mM boric acid, 0.2 mM Na_2EDTA) followed by autoradiography.

Relative Rate. Following the procedure detailed above, Eppendorf tubes containing 5′ end-labeled w794 DNA (9 μL) in TE buffer (pH 7.5) were treated with (+)-duocarmycin SA or (−)-duocarmycin SA (1 μL, 10^{-5} M in DMSO). The solutions were mixed and incubated at 25 °C for 1, 3, 6, 12, 24, 48, 96, and 192 h, respectively. Subsequent isolation of the alkylated DNA by EtOH precipitation, resuspension in TE buffer (10 μL, pH 7.5), thermolysis (30 min, 100 °C), concurrent PAGE, and autoradiography were conducted as detailed above. A relative rate of $k(+)/k(-) = 48$ for the (+)-**1** alkylation at the 5′-AATT<u>A</u> site ($k(+)$) versus (−)-**1** alkylation at the 5′-A<u>A</u>TTT site ($k(-)$) was derived from the slopes of the plots of percent integrated optical density (IOD) of the high affinity alkylation site cleavage bands versus time, Figure 11.

Reversibility Studies. General procedures, the preparation of singly 5′ end-labeled double-stranded DNA, gel electrophoresis, and autoradiography were conducted according to procedures described in full detail.[29]

Preparation of Unlabeled Double-Stranded DNA–Agent Covalent Complex. M13 universal primer, 5′-d(GTAAAACGACGGCCAGT), was annealed to the template in a small Eppendorf tube containing a solution of the single-stranded M13mp10 clone (w794/w836,[29] ca. 5 μg in 30 μL TE buffer), universal primer (5 μL, 3×10^{-4} $A_{260}/\mu L$), nick translation buffer (7.5 μL, 500 mM Tris-hydrochloride, pH 7.2, 100 mM $MgSO_4$, 1 mM dithiothreitol, and 500 μg/mL bovine serum albumin) in H_2O (7.5 μL). The solution was warmed at 100 °C for 5 min before the heat source to the water bath was turned off, and the solution was allowed to cool to 25 °C over 3 h. The condensate containing the annealed primer–template duplex was collected by centrifugation. Six units of the Klenow fragment of DNA polymerase I were added and mixed well, followed by the addition of 16.8 μL of a solution containing dNTPs (2 mM each dATP, dGTP, dCTP, and dTTP) to initiate the chain extension of the primer. The DNA synthesis reaction mixture was incubated for 16 min at 47 °C before an additional aliquot (16.8 μL) of the dNTP mixture was added, and the mixture was maintained for an additional 16 min at 47 °C. The double-stranded DNA synthesis was stopped with the addition of EDTA (5 μL, 0.25 M), and the DNA precipitated with EtOH. The DNA pellet obtained upon centrifugation was dissolved in 10 μL of phosphate buffer (pH 7.4, 0.1 M NaH_2PO_4–Na_2HPO_4), and the DNA concentration was determined by UV measurement. This double-stranded DNA was treated with the agent in 1 μL of DMSO at a 1:10 agent:base-pair ratio. The reaction solution was mixed, briefly centrifuged, and subsequently incubated at 25 °C, 1 day (for **1**), 4 °C, 3 days (for **3**) or 25 °C, 3 days (for (+)-CC-1065). Unbound agent was

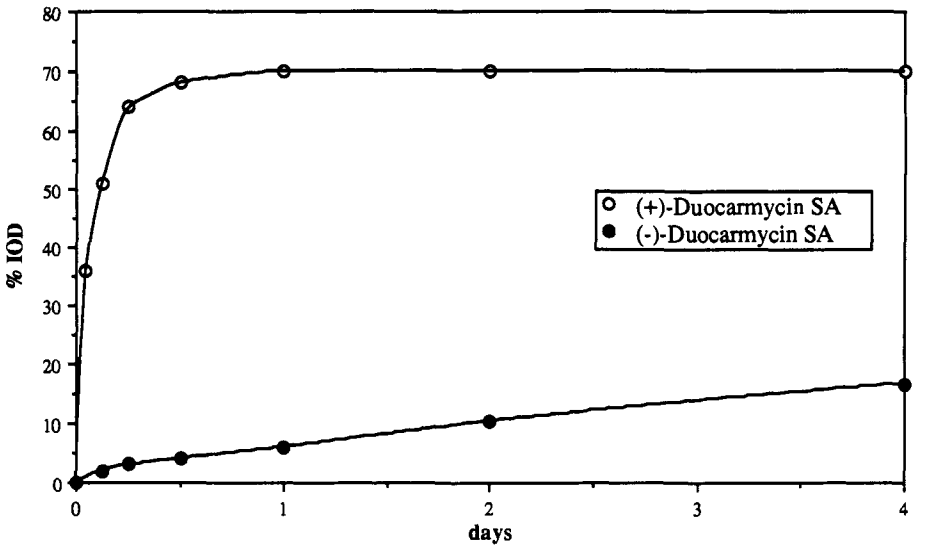

Figure 11. Plot of the percent integrated optical density (IOD) of 5′ end-labeled DNA derived from the alkylation and thermally-induced cleavage at the respective high affinity alkylation sites [5′-d(AATTA)-3′ for (+)-duocarmycin SA and 5′-d(AATTT)-3′ for (−)-duocarmycin SA, see Figure 7] within duplex w794 DNA versus time at 25 °C with 10^{-5} M agent. The optical density determinations were conducted on a BioImage Model 60S RFLP system.

removed by phenol extraction (1×), *n*-BuOH extraction (2×), and Et_2O extraction (1×). The residual Et_2O was removed under a stream of N_2, and the alkylated DNA was further purified and collected by EtOH precipitation.

Transfer of the Agent from Unlabeled w794/w836 DNA to Singly 5′ End-Labeled w794/w836 DNA. The agent·alkylated unlabeled duplex DNA from above was redissolved in aqueous buffer, mixed with ^{32}P singly 5′ end-labeled duplex w794/w836 DNA[29] at concentrations which represented 4:1, 1:1, and 0.5:1 molar ratios of unlabeled:labeled DNA, and incubated at 4–50 °C for 2 h to 8 days. The reaction was stopped by EtOH precipitation and isolation of the DNA. The DNA was resuspended in TE buffer (10 μL) followed by thermolysis at 100 °C for 30 min to induce cleavage at the alkylation sites. Formamide dye (5 μL) was added to the cooled mixture. Prior to electrophoresis, the samples were denatured by heating at 100 °C for 5 min, placed into an ice bath, centrifuged, and loaded onto the gel. Sanger dideoxynucleotide sequencing reactions were run as standards adjacent to the reaction samples. PAGE was carried out using an 8% sequencing gel under denaturing conditions (8 M urea) in TBE buffer and was followed by autoradiography. Quantitation through integrated optical density (IOD) determination of the unmodified labeled DNA and the alkylation site cleavage bands was conducted on a BioImage Model 60S RFLP system.

Time Dependence. The unlabeled double-stranded DNA–agent complex was dissolved in 55 μL of phosphate buffer (pH 8.4, 0.25 M NaH_2PO_4–Na_2HPO_4), and 5′ end-labeled double-stranded DNA was dissolved in 220 μL of TE buffer (pH 8.0). Four-microliter aliquots of each of the DNA solutions above were added to a fresh tube, and an additional 4 μL of phosphate buffer (pH 8.4, 0.25 M NaH_2PO_4-Na_2HPO_4) was added. The reactions were mixed, briefly centrifuged, and subsequently incubated at 50 °C (for **3** and CC-1065) or 37 and 50 °C (for **1**). The reaction was stopped at time intervals of 2 h, 4 h, 8 h, 1 day, 2 days, 4 days, and 6 or 8 days. The removed reaction tubes were stored at −20 °C before concurrent subjection of the samples to the thermal cleavage reaction, PAGE, and autoradiography.

Temperature Dependence. The temperature dependence experiment was conducted using the same procedure described above for the time dependence experiment. The samples were incubated at 50, 37, 25, and 4 °C for 4 days before being subjected to the thermal cleavage reaction, PAGE, and autoradiography.

Ionic Strength. The unlabeled double-stranded DNA–agent complex and 5′ end-labeled double-stranded DNA were dissolved in 55 and 220 μL of TE buffer (pH 8.0), respectively. Four-microliter aliquots of each of the DNA solutions above were added to a fresh tube, and aqueous 0.8 M NaCl (8, 4, 2, 1, or 0 μL) was added to each tube. The reaction mixtures were diluted with the addition of 0, 4, 6, 7, or 8 μL of TE buffer, respectively, to provide a final NaCl concentration of 400, 200, 100, 50, and 0 mM. The mixtures were incubated at 37 °C for 4 days before being subjected to the thermal cleavage reaction, PAGE, and autoradiography.

pH Dependence. A 4-μL aliquot of unlabeled double-stranded DNA–agent complex in 55 μL of phosphate buffer (pH 8.4, 0.25 M NaH_2PO_4-Na_2HPO_4) and a 4-μL aliquot of 5′ end-labeled double-stranded DNA in 220 μL of TE buffer were added to a fresh tube. The mixture of DNA was precipitated and collected with the addition of EtOH and redissolved in 10 μL of pH 6.0, 7.4, or 8.4 phosphate buffer (0.25 M NaH_2PO_4–Na_2HPO_4), respectively. The samples were incubated at 50 °C for 4 days before being subjected to the thermal cleavage reaction, PAGE, and autoradiography.

Isolation, Characterization, and Quantitation of the Thermally Released (+)-Duocarmycin SA–Adenine Adduct 4. (+)-Duocarmycin SA (**1**, 2.2 mg, 4.6 μmol) in 1.2 mL of DMF was added to a solution of calf thymus DNA[38] (Sigma, 200 mg, *ca.* 70 bp equiv) in 10 mM sodium phosphate buffer (30 mL, pH 7.0). The mixture was shaken for 24 h at 25 °C. The solution was extracted with EtOAc (2 × 10 mL) to remove unreacted or hydrolyzed **1**. UV assay of the EtOAc extracts revealed no unreacted (+)·**1**. A 50-mL centrifuge tube containing the aqueous DNA layer was sealed with Teflon tape and warmed at 100 °C for 25 min. The resulting solution was cooled to 25 °C and extracted with EtOAc (3 × 10 mL). The combined organic layer was dried (Na_2SO_4) and concentrated under reduced pressure to afford a yellow solid. Chromatography (SiO_2 pretreated with 5% Et_3N–CH_2Cl_2 and CH_2Cl_2, 0.5 × 6 cm, 0–10% MeOH–CH_2Cl_2 gradient elution) afforded the adduct (+)-**4** as a pale yellow solid (2.9 mg, 2.9 mg theoretical, 100%, 90–100% in three runs) contaminated with a small impurity (2–5% by HPLC). An analytically pure sample of protonated **4** was obtained by recyrstallization through slow evaporation of DMSO under reduced pressure (0.1 mmHg): mp 200 °C dec (DMSO, colorless needles), concentration dependent $[\alpha]^{23}_D$ +19 (*c* 0.062, CH_3OH), +36 (*c* 0.025, CH_3OH); R_f 0.25 (SiO_2, 10% CH_3OH–$CHCl_3$); ^1H NMR (400 MHz) given in Table 3 and Figure 3; ^{13}C NMR (100 Mz) given in Table 4; IR (film) ν_{max} 3352 (br), 3261 (br), 2916, 2848, 1701, 1654, 1528, 1438, 1315 cm^{-1}; UV (CH_3OH) 325 (sh, ε 22 000), 306 nm (ε 29 000); CD (CH_3OH) $[\theta]^{23}$ 326 (+18 300), 303 (−7300), 268 nm (+85 800); FABHRMS (NBA) *m/e* 613.2159 (M^+ + H, $C_{30}H_{28}N_8O_7$ requires 613.2159).

The 2D ^1H–^1H NMR (DMSO·d_6, 400 MHz) displayed NOE crosspeaks between N1-H (11.76 ppm) and C6-OH (9.92 ppm), C6-OH (9.92) and C7-H (7.71), Ade-N$H_a$$H_b$ (9.12) and Ade-N$H_a$$H_b$ (8.86), Ade-C2-H (8.46) and C13-H_a (4.71), Ade-C2-H (8.46) and C13-H_b (4.60), Ade-C2-H (8.46) and C10-H (4.24) (weak), C3′-H (6.88) and C11-H (4.52), C9′-H (6.88) and OCH_3 (3.80), C3-H (6.75) and C13-H (4.71), and C3-H (6.75) and C10-H (4.24). The 2D ^1H–^1H NMR (CD_3·OD, 400 MHz) displayed NOE crosspeaks between Ade-C2-H (7.73 ppm) and C13-$H_{a,b}$ (4.85 and 4.70 ppm), C9′-H (6.94) and OCH_3 (3.88), C3′-H (6.89) and C11-$H_{a,b}$ (4.73 and 4.59), C3-H (6.68) and C10-H (4.22), C13-H_a (4.85) and C13-H_b (4.70), and C11-H_a (4.73) and C11-H_b (4.59). The ^1H NMR assignments of Ade-C2-H, C3′-H, C3-H, C9′-H, C13-H, and C11-H in acetone-d_6 were based on the following NOEs (2D ^1H–^1H ROESY, 500 MHz): Ade-C2-H (8.12 ppm) and C13-H_a (4.89 ppm), Ade-C2-H (8.12) and C13-H_b (4.67), Ade-C2-H (8.12) and C10-H (4.55) (weak), C3′-H (6.97) and C11-H_a (4.82), C3′-H (6.97) and C11-H_b (4.61), C3-H (6.97) and C10-H (4.55), C3-H (6.97) and C13-H_a (4.89) (weak), C3-H (6.97) and C13-H_b (4.67) (weak), and

C9′-H (6.89) and C13′-OCH_3 (3.85). The 2D phase-sensitive (TPPI) NOESY experiment was run with 500-ms mixing time, 8064-Hz spectral width, 130-ms acquisition time, 2-s relaxation delay, 512 increments (data points) in the t_1 dimension, and 16 scans per increment. The data were processed using the Felix program with a 60-deg-shifted sinebell square function in the t_2 dimension and a 90-deg-shifted sinebell function in the t_1 dimension. The sample was deoxygenated by one freeze–pump–thaw cycle with argon purging.

Isolation, Characterization, and Quantitation of the Thermally Released (–)-Duocarmycin SA–Adenine Adduct 4. (–)-Duocarmycin SA ((–)-**1**, 1.0 mg, 2.1 μmol) in 50 μL of DMF was added to a solution of calf thymus DNA[38] (Sigma, 192 mg, *ca.* 100 bp equiv) in 10 mM sodium phosphate buffer (15.0 mL, pH 7.0). The mixture was incubated for 3 days at 25 °C. The solution was extracted with EtOAc (3 × 5 mL). Concentration of the organic extract provided (–)-**4** (6%) and no recovered unreacted **1** (UV quantitation). A centrifuge tube containing the aqueous DNA layer was sealed with Teflon tape and warmed at 100 °C for 30 min. The resulting solution was cooled to 25 °C and extracted with EtOAc (4 × 5 mL), and the combined organic layer was concentrated under reduced pressure. Chromatography (SiO_2, 0.5 × 6 cm, 0–10% CH_3OH–CH_2Cl_2 gradient elution, CH_2Cl_2 was passed through a column of basic Al_2O_3 prior to chromatography) afforded (–)-**4** as a white solid (1.1 mg, 1.8 μmol, 86%, combined yield of 92%) as the only UV active material (TLC, SiO_2) present in the crude or purified product, which proved to be identical in all respects to (+)-**4** but with the opposite optical and chiroptical properties: concentration-dependent $[\alpha]^{25}_D$ –24 (*c* 0.045, CH_3OH), –50 (*c* 0.018, CH_3OH); R_f 0.25 (SiO_2, 10% MeOH–$CHCl_3$); ^1H NMR (CD_3OD, 400 MHz) given in Table 3 and Figure 3; HPLC[47] t_R 26.4 min (VYDAC C18, 5 μm, 0.46 × 25 cm, 10–50% CH_3CN–0.05 M HCO_2-NH_4 linear gradient, 0–30 min, 1.0 mL/min); UV (CH_3OH) 325 (sh, ε 22 000), 306 nm (ε 29 000), UV (EtOAc) 332 (ε 22 000), 306 nm (ε 29 000); CD (CH_3OH) mirror image of (+)-**4** CD spectrum; FABHRMS (glycerol) *m/e* 613.2161 ($M^+ + H$, $C_{30}H_{28}N_8O_7$ requires 613.2159).

Acknowledgment. We gratefully acknowledge the financial support of the National Institutes of Health (CA55276) and the award of an ACS Organic Division fellowship sponsored by ZENECA pharmaceuticals to D. S. Johnson. We wish to thank Christine Tarby for her patient assistance in the molecular modeling studies and for developing the model rationalizing the distinguishing features of the enantiomeric pairs, D. L. Hertzog for providing the synthetic agents employed in our studies, and D. H. Huang for assistance in securing the 2D ^1H–^1H NMR spectra.

Supplementary Material Available: AMBER force field parameters for duocarmycin SA and A (6 pages). This material is contained in many libraries on microfiche, immediately follows this article in the microfilm version of the journal, and can be ordered from the ACS; see any current masthead page for ordering information.

(47) HPLC t_R of (+)-**4** and (–)-**4** were identical under all conditions and the analysis was carried out on a Waters HPLC unit (501 pumps, 994 programmable photodiode array detector) equipped with a VYDAC C18 column (5 μm, 0.46 cm × 25 cm). Detection was carried out at 254 nm with concurrent monitoring at 300 and 335 nm.